

Temporal distribution and diversity of cold-water corals in the southwest Indian Ocean over the past 25,000 years

Pratt Naomi ^{1,*}, Chen Tianyu ^{2,3}, Li Tao ^{2,3}, Wilson David J. ^{1,4}, Van De Flierdt Tina ¹, Little Susan H. ¹, Taylor Michelle L. ⁵, Robinson Laura F. ², Rogers Alex D. ^{6,7}, Santodomingo Nadiezhda ⁸

¹ Department of Earth Science and Engineering, Imperial College London, South Kensington Campus, Exhibition Road, London, SW7 2AZ, UK

² School of Earth Sciences, University of Bristol, BS8 1RJ, UK

³ School of Earth Sciences and Engineering, Nanjing University, Nanjing, 210023, China

⁴ Department of Earth Sciences, University College London, WC1E 6BS, UK

⁵ School of Biological Sciences, University of Essex, Wivenhoe Park, Colchester, CO4 3SQ, UK

⁶ Department of Zoology, University of Oxford, Tinbergen Building, South Parks Road, Oxford, OX1 3PS, UK

⁷ REV Ocean, Oksenøyveien 10, NO-1366, Lysaker, Norway

⁸ Natural History Museum, Department of Earth Sciences, Cromwell Road, SW7 5BD, London, UK

* Corresponding author : Naomi Pratt, email address : nrp15@ic.ac.uk

Abstract :

Fossil cold-water corals can be used to reconstruct physical, chemical, and biological changes in the ocean because their skeleton often preserves ambient seawater signatures. Furthermore, patterns in the geographic and temporal extent of cold-water corals have changed through time in response to environmental conditions. Here we present taxonomic and dating results from a new collection of subfossil cold-water corals recovered from seamounts of the Southwest Indian Ocean Ridge. The area is a dynamic hydrographic region characterised by eastward flow of the Agulhas Return Current and the northernmost fronts of the Antarctic Circumpolar Current. In total, 122 solitary scleractinian corals and 27 samples of colonial scleractinian material were collected from water depths between 172 and 1395 m, corresponding to subtropical waters, Antarctic Intermediate Water (AAIW), and Upper Circumpolar Deep Water (UCDW). Fifteen species were identified, including eight species new to the region. The assemblage reflects the position of the seamounts in a transition zone between Indo-Pacific and Subantarctic biogeographic zones. Morphological variation in caryophyllids and the restriction of dendrophylliids to the southern seamounts could result from genetic isolation or reflect environmental conditions. Uranium-series dating using both rapid laser ablation and precise isotope dilution methods reveals their temporal distribution from the Last Glacial Maximum to the present day. Only one specimen of glacial age was found, while peaks in abundance occur around Heinrich Stadial 1 and the Younger Dryas, times at which ocean chemistry and food supply were likely to have presented optimal conditions for cold-water corals. A widespread regional preference of cold-water corals for UCDW over AAIW depths during the deglacial, the reverse of the modern situation, could be explained by higher dissolved oxygen concentrations and a temperature inversion that persisted into the early Holocene.

Highlights

- ▶ First described southern Indian Ocean subfossil cold-water coral collection.
- ▶ Eight new species to the region identified.
- ▶ Dated using rapid laser ablation and isotope dilution uranium series techniques.
- ▶ Abundance peak during late deglacial a possible response to optimal ocean chemistry.
- ▶ Striking similarities in temporal distribution to other Southern Ocean collections.

43 **1. Introduction**

44 **1.1 Cold-water corals**

45 Cold-water corals (henceforth CWCs) comprise non-symbiotic (azooxanthellate) cnidarian
46 species of the orders Scleractinia, Octocorallia, Stylasteridae, and Antipatharia (Roberts et al.,
47 2009). About half of all species of scleractinian corals are azooxanthellate, some of which
48 can build structural habitats that provide refuge for many other species, although the majority
49 are solitary or free-living (Roberts et al., 2009). Most species of scleractinian CWCs are

50 found in ocean temperatures that range from 1 to 20°C (Stanley and Cairns, 1988) at shallow
51 to lower bathyal depths, with occasional records as deep as 6328 m (Keller, 1976).

52 Cold-water corals are particularly useful for unravelling changes in ocean biogeochemistry
53 and circulation in the past (Robinson et al., 2014). They are found in abundance in the
54 Southern Ocean, where other proxy archives such as foraminifera are sparse, and they can be
55 preserved on the seafloor or within sediments for thousands of years (e.g. Burke et al. 2010;
56 Margolin et al. 2014; Thiagarajan et al. 2013). Their depth range often covers intermediate
57 and deep water masses, complementing and extending records from abyssal sediment cores.
58 A record of seawater chemistry throughout their lifetime can be preserved in their carbonate
59 skeleton (Robinson et al., 2014), and their high uranium content allows for application of
60 precise uranium-thorium dating methods (Cheng et al., 2000a; Douville et al., 2010;
61 Lomitschka and Mangini, 1999; Montero-Serrano et al., 2013; Shen et al., 2012, 2008).

62 The physiology of CWCs and their response to environmental stressors is understudied in
63 comparison to their shallow-water counterparts. However, research volume has grown in
64 recent years, in part because of concerns about the impact of human activity on CWC
65 ecosystems (Guinotte et al., 2006). Water temperature is thought to be one of the most
66 important controls on their range at a global scale (Davies and Guinotte, 2011), but responses
67 to thermal stress have been shown to vary by species (e.g. Büscher et al., 2017; Gori et al.,
68 2016). Cold-water corals rely on a food supply of zooplankton, algal material and particulate
69 organic matter (Duineveld et al., 2007). Hydrography plays an important role in controlling
70 supply of this nutrition, as well as in the dispersal of larvae (Dullo et al., 2008; Miller et al.,
71 2010). Although dissolved oxygen is crucial for corals to maintain aerobic function, the limit
72 of tolerance is unknown, with colonies of the coral *Desmophyllum pertusum* (formerly known
73 as *Lophelia pertusa*) being found to survive at dissolved oxygen concentrations well below
74 the limit suggested in laboratory experiments (Dodds et al., 2007). The extent to which
75 carbonate ion concentration controls CWC range is also disputed. Although 95% of

76 branching CWCs are found above the aragonite saturation horizon (ASH; Guinotte et al.,
77 2006), recent expeditions have also recovered scleractinians from undersaturated waters (e.g.
78 Baco et al., 2017; Thresher et al., 2011). Regional fluctuations in seawater chemistry,
79 productivity, and water mass structure at times in the past are therefore all likely to have
80 exerted some control on regional habitat suitability for CWCs.

81 **1.2 The deglacial Southern Ocean**

82 In this study, we characterise and date a collection of subfossil CWCs from the southern
83 Indian Ocean for the first time and explore the environmental controls on their distribution
84 since the Last Glacial Maximum (LGM; ~23-19 ka). At this time, atmospheric CO₂
85 concentrations were 80-90 ppm lower than preindustrial values (Monnin et al., 2001).
86 Enhanced carbon storage in the deep ocean resulted from a more effective biological pump
87 (e.g. Wang et al., 2017) and reduced ventilation due to sea ice-induced stratification and/or
88 equatorward wind shifts (Ferrari et al., 2014; Kohfeld and Chase, 2017; Stephens and
89 Keeling, 2000). During the subsequent deglaciation, degassing of CO₂ from the deep ocean is
90 thought to have been responsible for the co-variation in atmospheric CO₂ and Antarctic
91 temperature change (Parrenin et al., 2013), characterised by two ‘pulses’ of CO₂ release
92 separated by a cooling and stabilisation of atmospheric CO₂ during the Antarctic Cold
93 Reversal (ACR; 14.5-12.7 ka; Stenni et al., 2011). Radiocarbon records indicate intervals of
94 breakdown in the deep vertical stratification (Burke and Robinson, 2012; Chen et al., 2015a;
95 Siani et al., 2013), while changes in pH conditions reflecting outgassing of CO₂ sourced from
96 deep waters have been reconstructed using boron isotopes (Martínez-Botí et al., 2015; Rae et
97 al., 2018).

98 The Indian sector of the Southern Ocean is an important location in which to study deglacial
99 ocean biogeochemistry. Frontal movements in this region may have led to changes in the
100 ‘leakage’ of warm, salty eddies from the Agulhas retroflexion into the Atlantic Ocean, with

101 implications for Atlantic overturning circulation (e.g. Bard and Rickaby, 2009; Beal et al.,
102 2011; Franzese et al., 2006). In addition, a lag between atmospheric cooling over Antarctica
103 during the ACR (Stenni et al., 2001) and sea surface temperature decline in the southern
104 Indian Ocean (Labracherie et al., 1989) has yet to be fully explained. To date, our
105 understanding of these changes and their global significance has been limited by sparse proxy
106 records from this region, motivating efforts to explore CWCs as a palaeoceanographic
107 archive. By taxonomically cataloguing and dating a new regional sample of intermediate-
108 water CWCs, this study provides a first step towards investigating these processes.

109 **2. Materials and methods**

110 **2.1 Sampling location and regional hydrography**

111 Subfossil corals were collected from four seamounts along the Southwest Indian Ocean Ridge
112 (SWIOR), which were surveyed in 2011 during expedition JC066 of the *RV James Cook*.
113 From south to north these were: Coral Seamount (41°21'23" S, 42°50'31" E); Melville Bank
114 (38°31'56" S, 46°45'74" E); Middle of What Seamount (henceforth 'MoW Seamount';
115 37°56'76" S, 50°22'16" E); and Atlantis Bank (32°42'01" S, 57°17'26" E; Fig. 1A; Table 1).

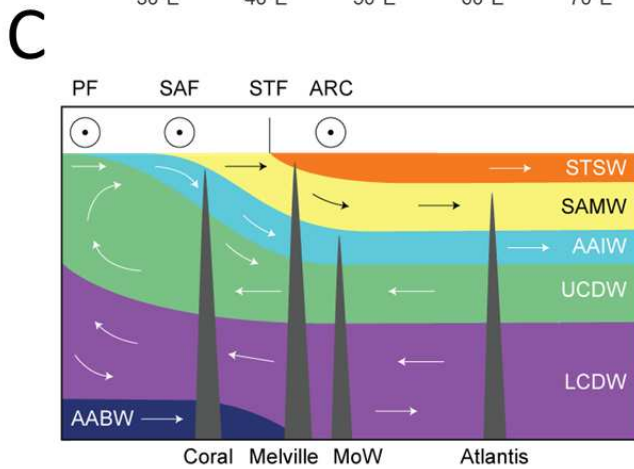
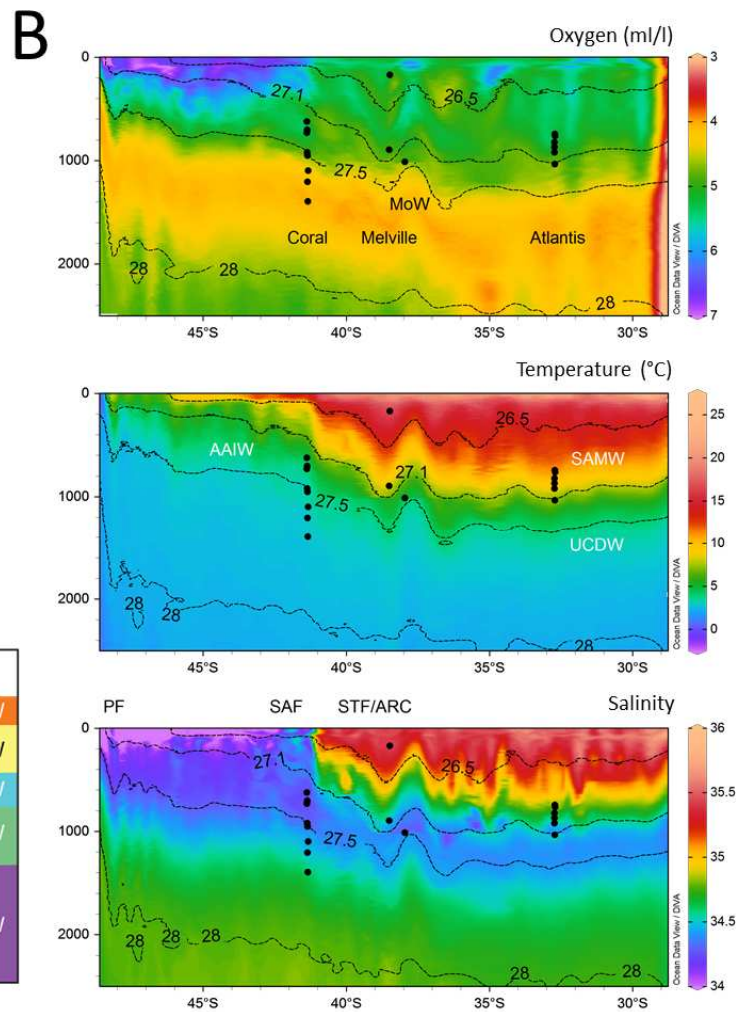
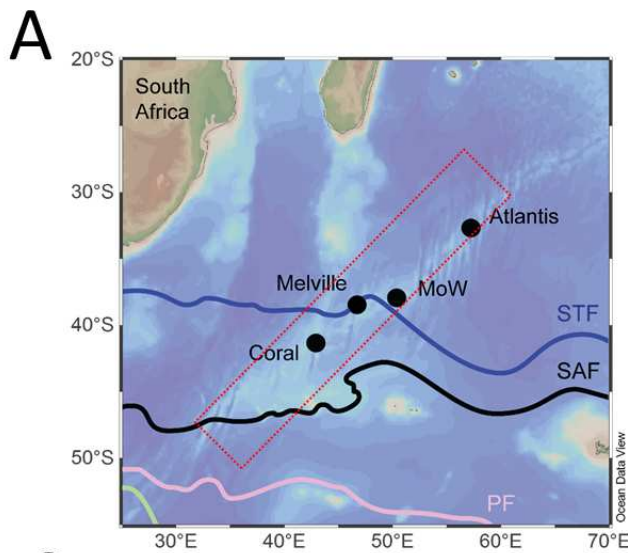
116 The modern Southwest Indian Ocean (SWIO) is dominated by two major hydrographic
117 features, the Antarctic Circumpolar Current (ACC) and the Agulhas Current system. The
118 Subantarctic Front (SAF), the northernmost front of the ACC, is strongly steered by
119 bathymetry in the SWIO (e.g. Pollard et al., 2007), resulting in a latitude range of 48-43°S
120 (Sokolov and Rintoul, 2009a; Fig. 1A). Further north, a 4°C increase in temperature and a
121 sharp increase in salinity (Fig. 1B) marks the position of the Subtropical Front (STF), the
122 boundary between subantarctic and subtropical surface waters, at around 40°S (Read and
123 Pollard, 2017). The eastward flowing Agulhas Return Current (ARC), which results from
124 overshoot and retroflexion of the Agulhas Current south of the African continent, is found in
125 close proximity to the STF in the SWIO (Belkin and Gordon, 1996; Lutjeharms and Van

126 Ballegooyen, 1988; Read and Pollard, 2017; Fig. 1B). Peak chlorophyll concentrations are
127 found at the ARC/STF, but the highest surface particulate organic carbon concentrations and
128 microorganism abundances are found between the two fronts, in the Subantarctic zone (SAZ;
129 Djurhuus et al., 2017b).

130 Density surfaces rise upwards to the south, in geostrophic balance with the eastward flow of
131 the ACC, affecting the depth at which specific water masses are present across the SWIO
132 transect (Fig. 1B, C). The subsurface salinity minimum of Antarctic Intermediate Water
133 (AAIW) is found between 500m (Coral) and 1500m (Atlantis) in the southern Indian Ocean
134 and was sampled at all seamounts (Fig. 1B, C). Upper Circumpolar Deep Water (UCDW), a
135 high-nutrient water mass consisting of a combination of Indian and Pacific deep waters, with
136 its upper bound defined by the 27.5 kg m^{-3} neutral density surface (Plancherel, 2012),
137 intersected with sampling at Coral (~900 m) and MoW (~1050 m) seamounts. Lower
138 Circumpolar Deep Water is found in the SWIO at depths of 2 to 3 km (van Aken et al., 2004;
139 Fig. 1C), but such depths were not sampled during this study.

140 Sampling was opportunistic and not all fossil CWCs seen were collected. All but three of the
141 specimens described here were collected during dives of the *Kiel 6000* Remotely Operated
142 Vehicle (ROV), using manipulator arms, a suction sampler, nets and mini-box corers (Rogers
143 and Taylor, 2011). The remaining specimens were extracted from a megacore sample
144 (JC066_1116), a boxcore sample (JC066_115), and picked up on a dive of the HYBIS towed
145 camera system (JC066_4309). On each seamount, ROV dives were made along deep to
146 shallow transects to analyse the depth and spatial variation of benthic communities. Five
147 ROV dives took place at Coral Seamount, four at Melville Bank, two at MoW Seamount, and
148 three at Atlantis Bank. The 149 scleractinian samples in the collection, of which 122 were
149 solitary, cover a depth range of 172 to 1395 m.

150 Figure 1: Modern day hydrography proximal to sample locations on the Southwest Indian Ocean
151 Ridge (SWIOR). A, bathymetric map of the sampling region in the Southwest Indian Ocean with
152 positions of fronts marked from north to south: Subtropical Front (STF), Subantarctic Front (SAF),
153 Polar Front, (PF), Southern Antarctic Circumpolar Current Front (green), from Sokolov and Rintoul,
154 (2009). Sample locations are shown with black dots, and the red box highlights the transect along
155 which sections are plotted. B, vertical sections with sampling locations shown with black dots. CTD
156 data accessed from the World Ocean Database, plotted with Ocean Data View (Schlitzer, 2017). From
157 top to bottom are plotted oxygen, labelled with seamount names; temperature, labelled with water
158 masses Subantarctic Mode Water (SAMW), Antarctic Intermediate Water (AAIW) and Upper
159 Circumpolar Deep Water (UCDW); and salinity, labelled with the three regional fronts. The path of
160 the Agulhas Return Current (ARC) combines with the STF as it crosses the SWIOR. Contours of
161 neutral density surfaces (kg m^{-3}) corresponding to water mass boundaries are shown on all three
162 sections. C, schematic section of present-day circulation and positions of frontal jets of the Antarctic
163 Circumpolar Current in the Indian sector of the Southern Ocean. Water masses depicted in addition to
164 SAMW, AAIW and UCDW are subtropical surface waters (STSW); Lower Circumpolar Deep Water
165 (LCDW) and Antarctic Bottom Water (AABW).



166

167 2.2 Taxonomy

168 Taxonomic identifications of the scleractinian coral specimens were based on monographs
 169 which represent the most recent, extensive, and available documents on azooxanthellate
 170 Scleractinia. These include Cairns (1982; Antarctic and Subantarctic), Cairns and Keller
 171 (1993; SWIO), Cairns (1995; New Zealand), Cairns and Zibrowius (1997; Indonesia), Cairns
 172 (2000; Caribbean), Kitahara et al. (2010) and Cairns and Polonio (2013; Indonesia).

173 Discrepancies in the boundaries and number of biogeographical realms exist between studies
 174 of azooxanthellate Scleractinia (see Cairns, 2007) and more recent classifications using
 175 benthic marine species and oceanographic proxies (most recently Watling et al., 2013). For
 176 the purposes of this study, we use a combination of the two. Atlantis Bank, Melville Bank

177 and MoW Seamount fall within the Indian Lower Bathyal Province proposed by Watling et
178 al. (2013) and the South-West Indian Ocean (SWIO) region following the terminology of
179 Cairns (Cairns, 2007). The STF is designated as the northern boundary for the Subantarctic
180 realm in Cairns (Cairns, 2007), whereas Watling et al. (2013) use the Polar Front. Therefore,
181 Coral Seamount is located in the Subantarctic according to Cairns (Cairns, 2007), but in the
182 Indian Province following Watling et al. (2013). To acknowledge this difference, along with
183 the likelihood that the boundary is transitional, we place Coral Seamount in the ‘Subantarctic
184 Transition Zone’.

185 During taxonomic analysis, specimens were evaluated for preservation of aragonite (1 –
186 highly degraded to 5 – intact) and the relative accumulation of authigenic coating (0 – no
187 coating to 3 – fully coated). These qualitative metrics were combined into a ‘preservation
188 factor’, by subtracting coating from aragonite preservation (see Appendix 4).

189 **2.3 Laser ablation U-series dating**

190 A total of 122 solitary scleractinian samples were prepared for laser ablation uranium-series
191 age screening in the Bristol Isotope Group (BIG) facilities, following the method developed
192 by Chen et al. (2015) and Spooner et al. (2016). Twenty-one specimens, predominantly of the
193 genus *Balanophyllia*, were too delicate, small, or poorly preserved to proceed with laser
194 ablation dating. Coral samples of a minimum size of 2 x 1.5 mm were cut using a Dremel®
195 tool with a diamond blade, polished flat on one side using four increasingly fine grades of
196 sandpaper, and rinsed with deionised water (18.2 MΩ. cm). Visibly altered or discoloured
197 sections of aragonite were avoided. The samples were then mounted in batches of ~50 into
198 trough-shaped sample holders.

199 Auto-focussed and pre-programmed 1.1 mm line scans were ablated automatically using
200 ‘Chromium 2.1’ software linked to the Photon Machines Analyte G2 193 nm laser, which
201 was coupled to a Thermo Finnigan Neptune MC-ICP-MS. The low abundance isotope ²³⁰Th

202 was measured in sequence on a central ion counter, with ^{238}U measured simultaneously using
203 Faraday cups (Spooner et al., 2016). Tuning was carried out using NIST 610 glass in order to
204 maximise ^{230}Th signal intensity. An aragonite vein standard from the Salt Wash Graben,
205 Green River, Utah (VS001/1-A) was used to bracket every three samples. Measurements
206 consisted of 50 cycles for samples and bracketing standards, and background intensities were
207 measured for 25 cycles following each standard measurement. Anomalous signal spikes in
208 ^{230}Th were removed before calculation of mean isotope intensities, subtraction of the
209 background intensity, and calculation of the isotope ratios; however, such spikes were rarely
210 observed. Corrections for instrumental, elemental, and isotopic fractionation were applied
211 using bracketing standards. Ratios were used to determine sample age by iteratively solving
212 the age equation using the Newton-Raphson method (Kaufman and Broecker, 1965). Closed
213 system behaviour was assumed, and the known modern seawater $\delta^{234}\text{U}_i$ value of $147 \pm 7 \text{‰}$
214 (Reimer et al., 2009) was used in the calculation. Previous data indicates age corrections for
215 initial ^{230}Th based on ^{232}Th fall within the usual age uncertainties for this method (Robinson
216 et al., 2014; Spooner et al., 2016), and therefore no correction was made for detrital or
217 seawater Th contribution. Standard errors on the measured ratios, the background
218 measurements, and the errors on the isotope dilution MC-ICPMS isotope ratios of the
219 standards were combined and propagated through each stage of standard corrections
220 (Spooner et al., 2016). Final propagation of errors through the age equation was carried out
221 using a Monte Carlo technique, whereby random Gaussian distributions for each ratio are
222 generated and used to calculate a distribution of possible ages from which the final sample
223 ages and errors are determined. For deglacial age corals these errors range between 500 and
224 1500 years. The background level was typically 1 count per second, with deglacial corals
225 recording 10-20 cps.

227 Fifty-two subsamples including two full procedural duplicates for combined U, Th, Nd
228 chemistry (~ 0.6 to 5 g) were taken for precise isotope dilution U-series analysis. Physical
229 and chemical cleaning procedures followed the development and assessment of methods
230 performed before in the MAGIC group at Imperial College on cold-water corals (Crocket et
231 al., 2014; van de Fliedrt et al., 2010), building on methods developed by Cheng et al. (2000),
232 Lomitschka and Mangini (1999) and Shen and Boyle (1988). All samples were rigorously
233 physically cleaned with a Dremel tool, before undergoing a two-day oxidative-reductive
234 chemical cleaning process. In the BIG laboratory facilities at the University of Bristol,
235 cleaned coral fragments (~0.04 to 1.9g) were then dissolved and spiked with a ^{236}U - ^{229}Th
236 mixed spike calibrated to a 4.1‰ (2 σ) uncertainty, described further by Burke and Robinson
237 (2012). An iron co-precipitation procedure was utilised to separate trace metals from the
238 carbonate matrix, before U and Th fractions were separated and purified using anion
239 exchange chromatography using columns filled with an Eichrom pre-filter resin and 2 mL
240 Biorad analytical grade anion exchange resin 1-X8 (100-200 mesh).

241 Uranium and Th isotopes were measured on a Neptune MC-ICP-MS in the BIG laboratories.
242 Bracketing standards were used: for U, an international standard U112a, and for Th an in-
243 house standard 'SGS'. A 45ppb U112a standard solution was used to tune the Neptune prior
244 to U measurement, such that sensitivity for ^{238}U was ~ 250 V/ppm with a variation of < 2%,
245 and between 5 and 95% peak height measured 0.1 amu or less. To correct for mass bias,
246 U112a and SGS were used to bracket U and Th samples respectively. Using these bracketing
247 standards, the activity ratios $^{238}\text{U}/^{234}\text{U}$, $^{232}\text{Th}/^{230}\text{Th}$, $^{232}\text{Th}/^{229}\text{Th}$, and $^{230}\text{Th}/^{229}\text{Th}$ were
248 corrected for each sample. The isotopes ^{238}U , ^{236}U and ^{235}U were analysed in Faraday
249 collectors, and ^{234}U on an ion-counter, in measurements of 100 cycles. The low concentration
250 ^{229}Th and ^{230}Th isotopes were analysed on the secondary electron multiplier (SEM) by peak
251 jumping in measurements of 50 cycles. ^{236}U , added as a spike to the Th cut, was measured

252 concurrently on a faraday cup. The latter was used to normalise the $^{230}\text{Th}/^{229}\text{Th}$ ratio for
253 signal instability, by measuring $^{230}\text{Th}/^{236}\text{U}$ and $^{229}\text{Th}/^{236}\text{U}$ (Burke and Robinson, 2012; Chen
254 et al., 2015b). The wash solution (i.e. blank) was analysed before every sample run in 10
255 cycles and subtracted from all absolute values before calculating isotope ratios. Machine
256 accuracy was monitored by measuring Hu84.5 (U) and ThB (Th) standards before each
257 session and every 3-4 samples. An HU84.5 standard was processed with each batch of
258 column chemistry and yielded a long-term external reproducibility for [$^{230}\text{Th}/^{238}\text{U}$] of $0.997 \pm$
259 0.002 , and for [$^{234}\text{Th}/^{238}\text{U}$] of 1.0007 ± 0.0008 , within error of secular equilibrium (n=50).
260 Errors including machine uncertainties and procedural blanks were propagated into the
261 isotope ratios of $^{234}\text{U}/^{238}\text{U}$, $^{236}\text{U}/^{238}\text{U}$ and $^{229}\text{Th}/^{230}\text{Th}$. A Monte Carlo technique was used to
262 propagate the errors of isotope ratios into the final reported uncertainties.

263 The isotope ^{232}Th was measured in addition to ^{230}Th in order to correct for non-radiogenic
264 sources. Assuming any initial Th incorporated on calcification had a $^{230}\text{Th}/^{232}\text{Th}$ ratio
265 equivalent to local modern-day seawater, the measured ^{232}Th can be used to estimate initial
266 ^{230}Th . An initial atomic $^{232}\text{Th}/^{230}\text{Th}$ ratio of $12,500 \pm 12,500$ (2σ) was assumed,
267 corresponding to modern subtropical Atlantic intermediate waters (Chen et al., 2015). This
268 calculation dominates the final error for ages, with measured ^{232}Th correlating with the
269 sample age error due to the greater uncertainty of initial ^{230}Th activity. Measured ^{232}Th
270 ranged from 50 to 3806 ppt, and was the main factor determining the age errors, which
271 ranged from 68 to 985 years for deglacial age corals.

272 The value $\delta^{234}\text{U}_i$ is the deviation (%) from secular equilibrium of the $^{234}\text{U}/^{238}\text{U}$ activity ratio
273 and is used to test for closed-system behaviour of the corals. The $\delta^{234}\text{U}_i$ of the SWIO corals
274 ranged from 145.2 to 157.5 ‰. Two of the 50 corals analysed exhibited open-system
275 behaviour with $\delta^{234}\text{U}_i$ outside of the modern-day ocean (147 ± 7 ‰; Reimer et al., 2009).
276 Ages of the full procedural duplicates were within error.

278 **3.1 Taxonomy**

279 Material from colonial species accounts for 27 of the 149 scleractinian samples, including
280 *Solenosmilia variabilis*, *Madrepora oculata*, *Goniocorella dumosa*, and *Enallopsammia*
281 *rostrata*. *Solenosmilia variabilis* appears to be the most common species represented among
282 the colonial specimens. However, it is difficult to evaluate the relative abundance of these
283 species as the number of samples cannot be considered representative of the communities
284 found at each seamount.

285 Of the 122 solitary specimens, the majority represent the family Caryophylliidae, which
286 includes *Desmophyllum dianthus* ($n = 36$), and *Caryophyllia diomedea* ($n = 32$).
287 Dendrophylliids are also common, including *Balanophyllia gigas*, *Balanophyllia*
288 *malouinensis*, and *Leptopsammia stokesiana* ($n = 31$). The remaining solitary specimens
289 comprise 13 flabellids (*Flabellum flexuosum* and *Javania antarctica*), two attached
290 *Trochocyathus gordonii*, and free-living specimens of *Deltocyathus sp.* and *Dasmosmilia*
291 *lymani*. Five solitary and four colonial samples were not identified to genus level due to poor
292 preservation.

293 An annotated list detailing the 15 scleractinian taxa represented within the new collection is
294 presented below (with further metadata in Appendix 1).

295 *3.1.1 Species List*

296 Order SCLERACTINIA

297 Family **OCULINIDAE** Gray, 1847

298 1. *Madrepora oculata* Linnaeus, 1758. Four fragments of this colonial coral,
299 characterised by sympodial budding and anastomosed branches, were collected from patches
300 of coral rubble at Melville Bank and MoW Seamount.

302 2. *Caryophyllia diomedae* Marenzeller, 1904. Thirty specimens found at Coral
303 Seamount, MoW Seamount and Atlantis Bank shared a hexameral $S1=S2>S3\geq S4$ septal
304 pattern, low, evenly spaced costae, sinuous pali on S3, and a columella formed of fascicular
305 elements (Cairns, 1995; Cairns and Zibrowius, 1997; Kitahara et al., 2010). Two specimens
306 displayed an irregular septal pattern, with 43 and 44 septa in total; similar variations have
307 been described previously from the Atlantic (Zibrowius, 1980) and New Zealand (Cairns,
308 1995). At least eight specimens had fewer than three columella elements. A few specimens
309 from Atlantis Bank and one from MoW Seamount have highly exert S1-2, up to 5mm (Fig.
310 2A); however, in most specimens from Coral Seamount and Melville Bank S1-2 were only
311 moderately exert (Fig. 2B). This character arguably places the latter group closer to the range
312 of *Caryophyllia laevigata*, a species described by Kitahara et al. (2010). In this case, the
313 differences amongst specimens was not consistent enough to identify them as separate
314 species, rather than considering a wide range of morphological variation of *C. diomedae*.
315 Another diagnostic feature, colour banding, was variably expressed and did not necessarily
316 correlate with septal exertness. Finally, it is worth mentioning that most of the Atlantis Bank
317 specimens exhibit fused costal granules near the calicular margin.

318 3. *Caryophyllia profunda* Moseley, 1881. One specimen of this taxa was collected,
319 from Melville Bank (Appendix 5). Unlike specimens described by Cairns (1995, 1982), all
320 septal edges are straight.

321 4. *Trochocyathus (T.) cf. gordonii* Cairns, 1995. One specimen composed of two
322 budded coralla found at Coral Seamount was assigned to *T. cf. gordonii*, although poor
323 preservation, especially of the pali, hampers conclusive identification (Appendix 5). As in the
324 New Zealand specimens (Cairns, 1995), deep intercostal striae are present near calicular

325 edge, becoming less defined towards the pedicel. Both specimens have an irregular septal
326 arrangement approaching decamerall.

327 5. *Solenosmilia variabilis* Duncan, 1873. Fragments of *S. variabilis* were collected
328 from Coral Seamount and Melville Bank.

329 6. *Goniocorella dumosa* (Alcock, 1902). Fragments were found at Coral Seamount
330 only. Specimens display straight, cylindrical branches and right-angled budding as described
331 in Cairns (1982).

332 7. *Dasmosmilia lymani* (Pourtalès, 1871). One specimen was found at Coral
333 Seamount, having fewer columella components than described in Cairns (1995), but a similar
334 septal arrangement, budding pattern, and serrate calicular edge.

335 8. *Desmophyllum dianthus* (Esper, 1794). The most common species with a total of 36
336 specimens collected from Coral Seamount, Melville Bank, and Atlantis Bank. They exhibit a
337 wide range of variation within the species, from small juvenile to large adult specimens,
338 straight to slightly bent corallum, and low to highly exert septa. A few specimens from
339 Atlantis Bank are distinct in that they most clearly bear the characteristic features of *D.*
340 *dianthus*: clear, ridged costae; highly exert, flared septa and finely granular theca (Fig. 2C;
341 Cairns, 1982).

342 Family **DELTOCYATHIDAE** Kitahara et al., 2012

343 9. *Deltocyathus* sp. Milne Edwards and Haime, 1848. A single, small, free living
344 specimen was found at Melville Bank. The specimen exhibits diagnostic characters of the
345 genus *Deltocyathus*, having pali before septa of all but first cycle and axial edges of higher
346 septa (S4) joining to faces of adjacent septa (S3). However, the poor preservation of the
347 specimen hampers its identification to species level.

348 Family **FLABELLIDAE** Bourne, 1905

349 10. *Flabellum flexuosum* Cairns, 1982. Three specimens were collected at Coral
350 Seamount. They exhibit a thin, porcellaneous theca, and sinuous, wrinkled edges of the inner
351 septa (Cairns, 1982, Appendix 5). However, none have a fifth septal cycle.

352 11. *Javania antarctica* (Gravier, 1914). Seven specimens from Coral Seamount and
353 one from Melville Bank were collected. Although similar in morphology to *F. flexuosum*,
354 these specimens were distinguished by their distinctive chevron growth lines peaking at
355 intersections with 'costae', as described in Cairns (1982; Appendix 5). Only one specimen
356 displayed a rudimentary fifth septal cycle.

357 Family **DENDROPHYLLIIDAE** Gray, 1847

358 12. *Balanophyllia gigas* Moseley, 1881. Twenty-one specimens representing this
359 species were found at Coral Seamount. It is likely that all specimens are juvenile, as none
360 express a full Pourtalès plan septal arrangement and they are much smaller than specimens
361 described from New Zealand (Cairns, 1995). The presence of banded epitheca above the
362 synapcticulotheca (Cairns and Zibrowius, 1997) is variable. They all have in common a deep,
363 narrow fossa and relatively narrow septa (Appendix 5).

364 13. *Balanophyllia malouinensis* Squires, 1961. A total of five specimens were
365 recovered from Coral Seamount and Melville Bank. They were distinguished from *B. gigas*
366 by having a thick, spinose synapcticulotheca and a shallower fossa with a larger columella
367 (Cairns, 1982; Appendix 5). Like the *B. gigas* specimens, the septa are arranged only in a
368 rudimentary Pourtalès plan.

369 14. *Leptopsammia stokesiana* Milne Edwards and Haime, 1848. Five specimens were
370 found at Coral Seamount. Although similar in size and morphology to the other solitary
371 dendrophylliids in the collection, these do not have a Pourtalès plan septal arrangement
372 (Cairns and Zibrowius, 1997).

373

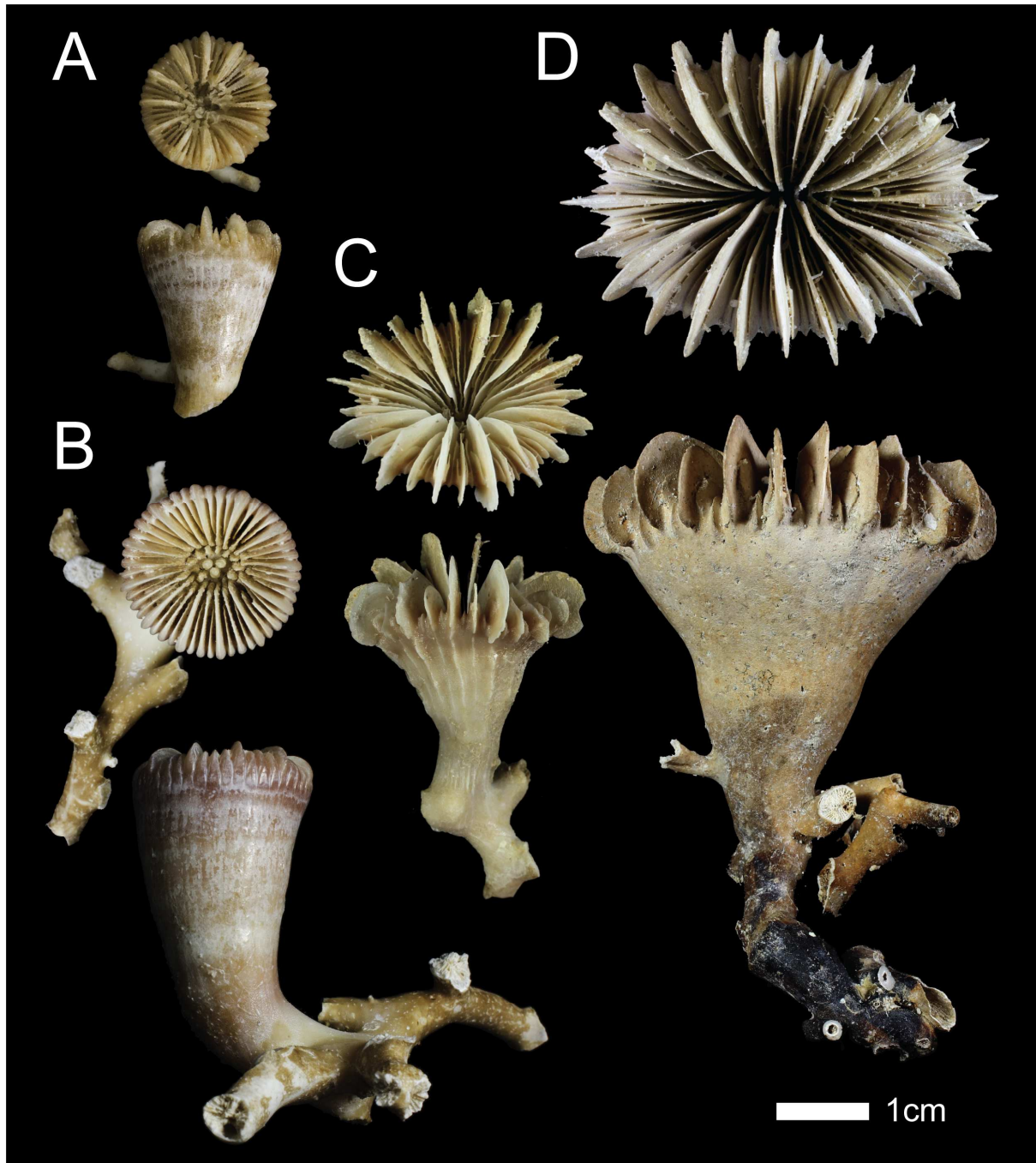
15. *Enallopsammia rostrata* (Pourtales, 1878). In total four fragments of this robust,

374

uniplanar colonial coral were found at Melville Bank and Atlantis Bank.

ACCEPTED MANUSCRIPT

375 **ACCEPTED MANUSCRIPT** Figure 2: Morphological variability of CWCs across seamount transect. Calice and corallum of
376 *Caryophyllia diomedea* from A, Atlantis Bank (JC066_3741) and B, Coral Seamount (JC066_122);
377 and calice and corallum of *Desmophyllum dianthus* from C, Atlantis Bank (JC066_3718) and D,
378 Coral Seamount (JC066_127).



379

380 3.1.2 Taxonomic distribution

381 All solitary CWCs except the *C. profunda*, which was collected at the summit of Melville
382 Bank at 172 m water depth, were found between 600 and 1400 m (Figs. 1, 3), covering

383 modern SAMW, AAIW, and UCDW depths, although the latter was only represented by
 384 specimens from Coral Seamount. This depth range is in part constrained by the position of
 385 the seamount summits, particularly at MoW Seamount (1100 m) and Atlantis Bank (750 m),
 386 and the maximum depth of the ROV surveys (see Table 1 and Fig. 3).

387 Table 1: Location, bathymetry, and number of specimens from SWIO seamounts

Seamount	Latitude (°S)	Longitude (°E)	Summit (m)	Max survey depth (m)	Solitary CWC specimens	CWC specimens dated
Coral	41°21'23" S	42°50'31" E	175	1395	89	72
Melville	38°31'56" S	46°45'74" E	91	1276	9	5
MoW	37°56'76" S	50°22'16" E	876	1414	7	7
Atlantis	32°42'01" S	57°17'26" E	690	1117	17	17

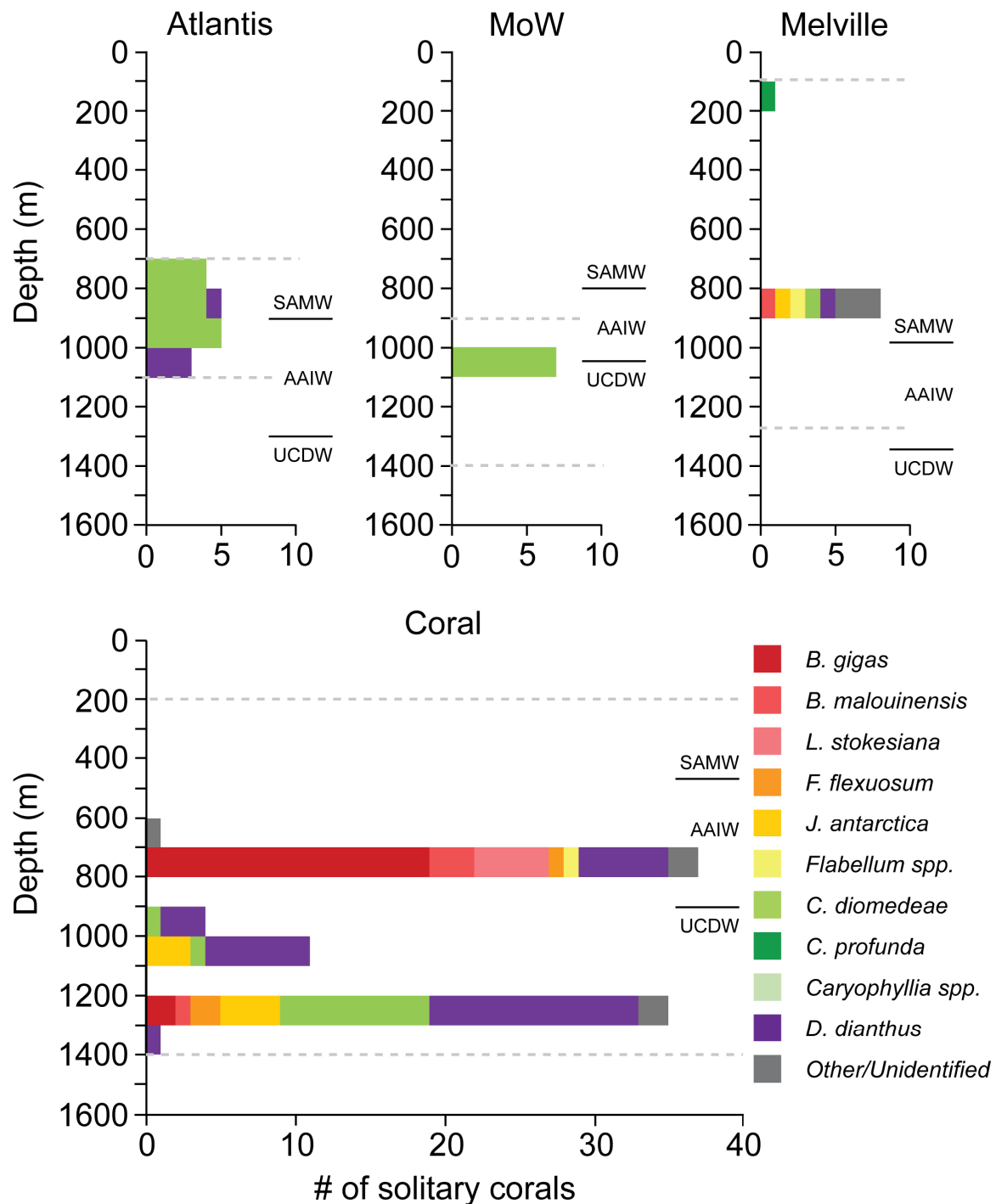
388
 389 At Coral Seamount, the greatest number ($n = 89$) and diversity of CWCs was found, with 9
 390 out of 11 solitary species represented (Fig. 3). Samples were collected between 624 and 1395
 391 m, intersecting the boundary between AAIW and UCDW at ~900 m. Most corals of this
 392 collection were recovered at ~700 m, where 27 of the 30 Dendrophylliidae specimens are
 393 found, and ~1200 m, dominated by Caryophylliidae.

394 At Melville Bank and MoW Seamount, solitary CWC specimens were found near to the
 395 modern-day SAMW/AAIW and AAIW/UCDW boundaries, respectively (Fig. 1B). Nine
 396 specimens from Melville Bank represent a minimum of five species (Fig. 3). All seven CWCs
 397 from MoW Seamount are *C. diomedae*. At both seamounts the ROV transect extended a few
 398 hundred metres below where the deepest CWCs were found.

399 The 17 CWC specimens from Atlantis Bank span the full depth range surveyed from 700 to
400 1100 m. *Desmophyllum dianthus* and *C. diomedea* were the only solitary species collected
401 in this locality (Fig. 3).

402 A range of preservation of the skeletal aragonite was observed, from near-perfect to heavily
403 bored and/or dissolved. Corals were often found coated with grey-brown authigenic deposits.
404 No significant correlation was found between water depth and individual coral mass or
405 preservation factor (Fig. 4A). On the whole, coating levels and aragonite degradation appear
406 to be positively correlated, i.e. poor aragonite preservation was linked to high coating levels
407 (see Appendix 4).

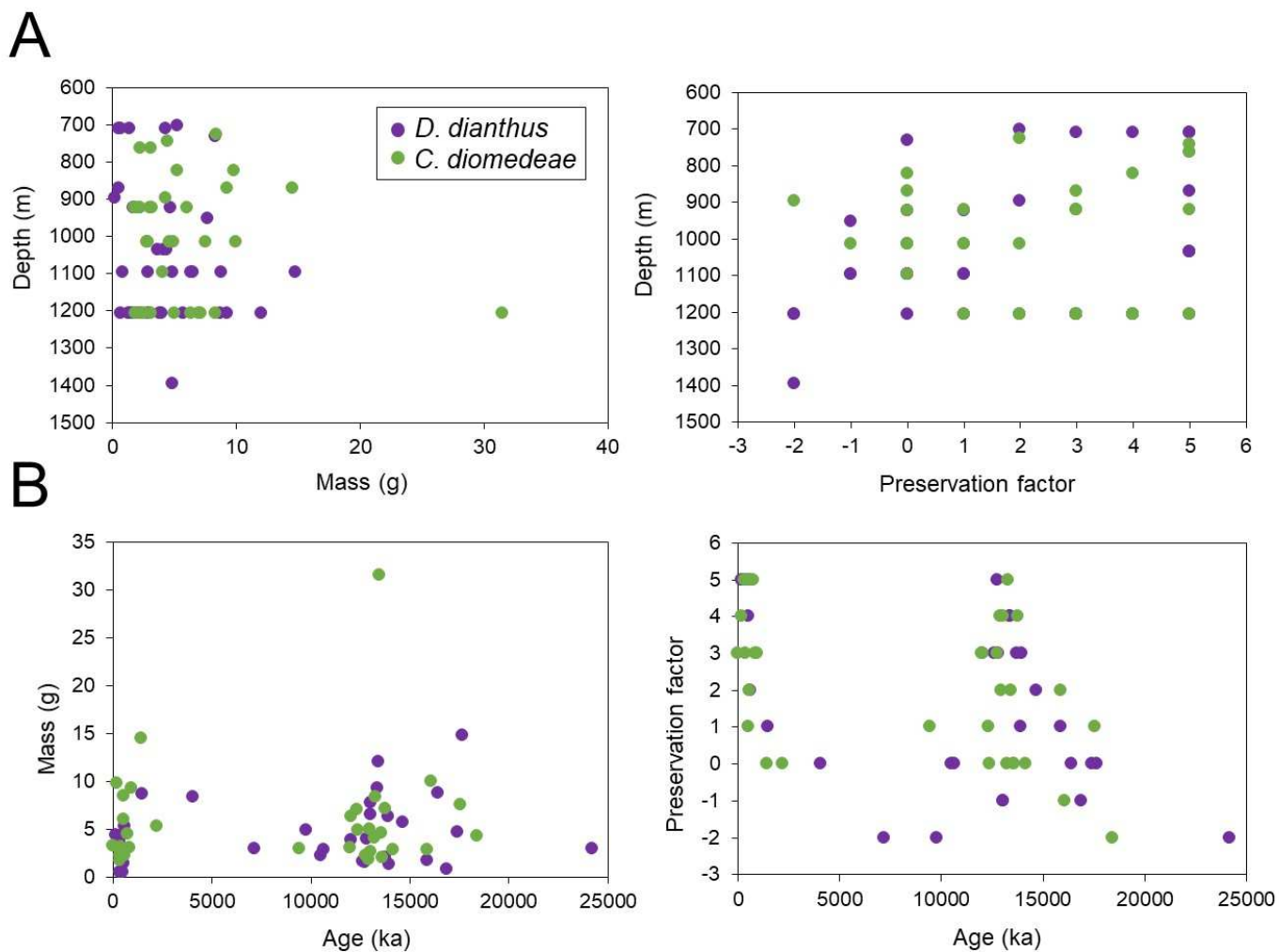
408 Figure 3: Depth distribution of subfossil CWCs at each seamount, colour coded by species. Seamount
 409 summits and the deepest vertical extent of ROV surveying are represented by dashed grey lines.
 410 Modern day water mass boundaries between Subantarctic Mode Water (SAMW), Antarctic
 411 Intermediate Water (AAIW) and Upper Circumpolar Deep Water (UCDW) are defined using the
 412 depths of neutral density for AAIW ($27.1 < \gamma_n < 27.5$; Plancherel, 2012) at each seamount, from World
 413 Ocean Database CTD data.



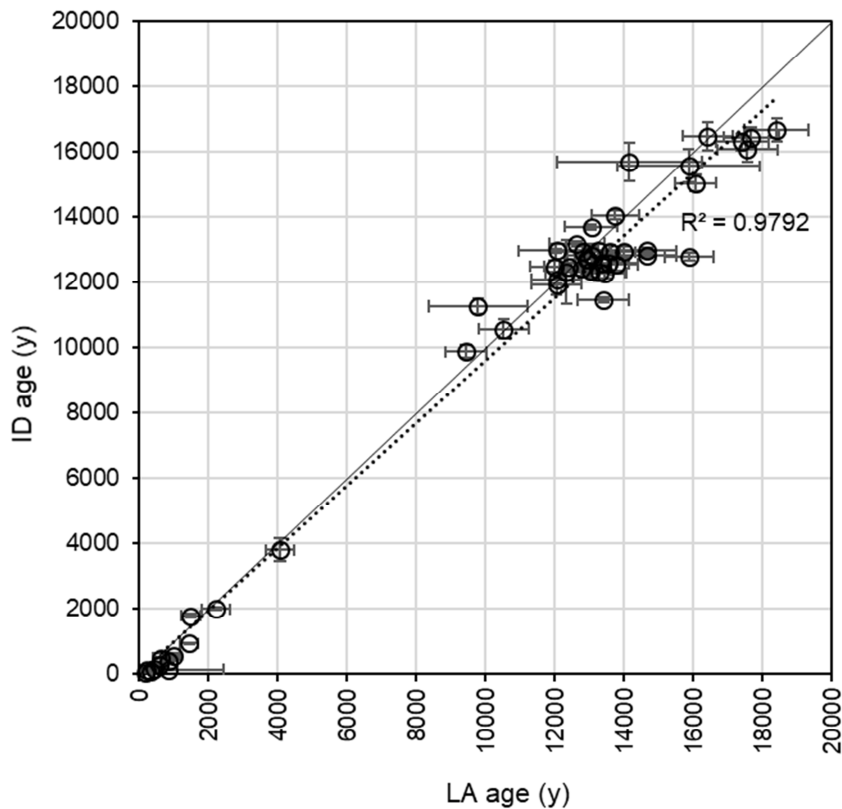
414

416 The 101 dated CWCs range in age from the LGM to the modern day (Fig. 6), except for a
417 single 140 ka specimen from Melville Bank. Isotope dilution U-series dating of 50 of the
418 samples demonstrated the accuracy of the laser ablation technique, with a close correlation
419 and 33 samples giving ages within error of the laser ablation dates (Fig. 5). Only late
420 Holocene CWCs were found at Atlantis Bank, whereas both Holocene and deglacial
421 specimens were found at Coral Seamount, Melville Bank and MoW Seamount. There are
422 relatively few samples from the mid-Holocene (~5 ka) and the Last Glacial Maximum (19 –
423 25 ka). The most well preserved and largest CWCs date from periods of greatest abundance,
424 whilst the few corals found during the LGM and early- to mid-Holocene are poorly preserved
425 (Fig. 4B).

426 Figure 4: Relationship of caryophylliid mass and preservation factor to A, depth and B, age, at all
 427 seamounts for the two most prevalent species (colour coded). Preservation factor is a qualitative
 428 metric that takes into account the amount of ferromanganese coating and aragonite dissolution, and
 429 ranges from -2 (least well preserved) to 5 (intact).



430
 431 Figure 5: Comparison of laser ablation (LA) and isotope dilution (ID) U-series ages for 50 cold-water
 432 corals from south-west Indian Ocean seamounts. The 1:1 line (solid) and trendline (dashed) are
 433 shown.



434

435 **4. Discussion**

436 **4.1 Taxonomy**

437 *4.1.1 Range extensions*

438 Previous surveys of CWC diversity in the region include the works of Cairns and Keller
 439 (1993) for southern Africa and Madagascar, and Cairns (1982) for the Antarctic and
 440 Subantarctic. In the former, the scleractinian fauna is described as having influence from
 441 Pacific, and to a lesser extent, Atlantic faunas, in addition to species endemic to the Indian
 442 Ocean. The distribution of the species in this collection and their proposed extensions are
 443 shown in Table 2. Of the 15 scleractinian deep-water coral species found in this study, six
 444 have already been recorded from the SWIO and/or Subantarctic regions: the cosmopolitan
 445 species *C. profunda*, *D. dianthus*, *M. oculata*, *E. rostrata* and *S. variabilis*, in addition to *G.*
 446 *dumosa*, which is Indo-West Pacific (Cairns and Keller, 1993; Cairns, 1982). The genus

447 *Deltocyathus* is also widely distributed in all oceans; although as we were not able to identify
448 the specimen to species level, future explorations and collection of well-preserved specimens
449 from these localities will be needed to allow a better knowledge of this genus in the region.
450 The remaining eight species represent extensions to their previously documented ranges
451 (Table 2), increasing the known scleractinian diversity of the SWIO and Subantarctic
452 Transition Zone. Surprisingly, none of the Dendrophylliidae or Flabellidae species described
453 previously from the SWIO (Cairns and Keller, 1993) were observed in this collection.
454 The connectivity of Indian and Pacific surface waters through the Indonesian throughflow led
455 Cairns and Keller (1993) to predict that representation of the 'Indo-West Pacific' fauna
456 would increase with further exploration in the SWIO. The first record of three species in the
457 Indian Ocean supports that prediction: *T. gordonii* (known only from the Kermadec Islands,
458 New Zealand / Kerguelen province; Cairns, 1995), *B. gigas* (West Pacific and New Zealand /
459 Kerguelen; Cairns and Zibrowius, 1997), and *D. lymani* (warm temperate Pacific and
460 Atlantic; Cairns, 2000). Connectivity of the Southern Ocean through the ACC could also
461 have contributed to the spread of these species. All three species were found at depths (700-
462 1200 m) which extend their bathymetric distribution to deeper waters (Table 2).
463 The seamounts cover a transitional biogeographic zone between the Indian and Subantarctic
464 regions, which is reflected both by the extension of species from the south into the Indian
465 province, and from temperate regions into the Subantarctic. Known previously only from the
466 Antarctic continent (Cairns, 1982), *F. flexuosum* was found north of the SAF at Coral
467 Seamount. There is evidence that genetic dispersal of CWCs follows ocean density gradients
468 and is less likely to occur vertically (Dullo et al., 2008; Miller et al., 2011). It is possible that
469 *F. flexuosum* extend their distribution up to the SWIO thanks to northwards transport via
470 intermediate waters, as it is found below its previously known depth range between 700 and
471 1200 m. *Javania antarctica* and *Balanophyllia malouinensis*, whose ranges were recently
472 extended from the Antarctic / Subantarctic (Cairns, 1982) to the southwest Atlantic (Cairns

473 and Polonio, 2013), were also found at Coral Seamount as well as Melville Bank. Water
474 temperature at Atlantis Bank may be above the tolerance of these Antarctic species. It is also
475 possible that the ARC acts as a dispersal barrier to the Indian Ocean for CWC larvae, in a
476 similar manner to the ACC (e.g. Dueñas et al., 2016); although to our knowledge this has not
477 yet been modelled or evaluated.

478 Neither *C. diomedea* nor *L. stokesiana* were listed in Cairns and Keller's (1993) SWIO
479 monograph, but both have been found previously in the Indian and West Pacific provinces
480 (Cairns and Zibrowius, 1997; Kitahara et al., 2010). As they were collected from Coral
481 Seamount, their ranges are extended into the Subantarctic Transition Zone. This find also
482 extends the range of *L. stokesiana* from shallow to bathyal waters.

Table 2: Distribution of subtropical and Subantarctic Transition Zone (TZ) south-west Indian Ocean (SWIO) and Indian Ocean (IO) Bathyal Province azooxanthellate Scleractinia discussed in this study. Depth range in bold signifies a proposed bathymetric extension. MoW: Middle of What seamount.

Species	TZ											SWIO			New record		
	Antarctic	Subantarctic	Coral Seamount	Melville Bank	MoW seamount	Atlantis Bank	Other SWIO sites	Indian	West Pacific	New Zealand / Kerguelen	Atlantic	Cosmopolitan	Depth (m) (worldwide)	SWIO <i>sensu</i> Cairns (1982)	IO Bathyal Province <i>sensu</i> Watling et al. (2013)	Subantarctic Transition Zone	
<i>Madrepora oculata</i>		x		x	x		x	x	x	x	x	55-1950					
<i>Caryophyllia diomedea</i>			x		x	x		x	x	x	x	225-2200	x		x		
<i>Caryophyllia profunda</i>	x	x		x			x	x		x		35-1116					
<i>Trochocyathus (T). gordoni</i>			x						x			398-732	x	x	x		
<i>Solenosmilia variabilis</i>	x	x	x	x			x	x	x	x	x	220-2165					
<i>Goniocorella dumosa</i>		x	x				x	x	x	x		88-1488					
<i>Dasmosmylia lymani</i>			x						x	x	x	37-1207	x	x	x		
<i>Desmophyllum dianthus</i>	x	x	x	x		x	x	x	x	x	x	8-2460					
<i>Deltocyathus sp.</i>				x			x	x	x			44-5080					
<i>Flabellum flexuosum</i>	x		x									101-1207	x	x	x		
<i>Javania antarctica</i>	x		x	x						x		53-1280	x	x	x		
<i>Balanophyllia gigas</i>			x						x	x		90-1200	x	x	x		
<i>Balanophyllia malouinensis</i>	x	x	x	x						x		75-1207		x			
<i>Leptopsammia stokesiana</i>			x					x	x			46-710	x		x		
<i>Enallopsammia rostrata</i>		x		x		x	x	x		x	x	110-2165					

1 4.1.2 *Spatial variability*

2 The seamounts in the SWIO form a transect across contrasting hydrographic and productivity
3 regimes, with peak chlorophyll concentrations nearest to the ARC/STF frontal zone (Melville
4 and MoW seamounts; Read et al., 2000). During the JC066 cruise, surface nutrient and
5 particulate organic carbon (POC) concentrations were found to be highest at Coral Seamount
6 (Djurhuus et al., 2017b), as was microorganism abundance (Djurhuus et al., 2017a). These
7 features, along with the systematic variability in microbial community structure, led Djurhuus
8 et al. (2017a) to separate the region into three biogeographic zones – south (Coral Seamount),
9 convergence zone (Melville Bank and MoW Seamount), and north (Atlantis Bank). At depth,
10 water masses were considered more influential, with similar taxa occurring below 200 m
11 across the seamounts (Djurhuus et al., 2017a). The limited sample size and opportunistic
12 nature of the sampling in this study makes a quantitative assessment of spatial variability
13 patterns in CWCs difficult. Because of the differing seamount heights, the maximum depth of
14 the ROV, and cruise time constraints (i.e. opportunistic sampling of subfossil CWCs), the full
15 depth range of CWCs may not have been surveyed (Table 1). Nevertheless, notable variations
16 in coral diversity are present in the dataset and warrant exploration.

17 Firstly, a larger number of samples and greater species diversity in subfossil Scleractinia was
18 found at Coral Seamount relative to the other seamounts (Fig. 3). This could be explained by
19 sampling bias, as ROV bottom time was approximately 35 hours at Coral, longer than at
20 Melville (~ 29 hrs), Atlantis (~ 26 hrs) and MoW (~11 hrs); at MoW sampling was severely
21 hampered by turbulent conditions. However, a wide variety of habitats was noted from video
22 footage at Coral Seamount (Rogers and Taylor, 2011), and video surveys suggest it hosts the
23 greatest diversity and number of species for corals and sponges (Frinault, 2017). It was also
24 found to host the largest microbial community (Djurhuus et al., 2017a) and the highest
25 surface chlorophyll concentrations of the four seamounts (Djurhuus et al., 2017b). There are
26 several factors which could contribute to the favourability of Coral Seamount as a habitat for

27 CWCs. As a result of its position south of the STF, water temperatures at Coral were ~ 3°C to
28 5°C at the depths of coral collection (~ 600 – 1400 m; Fig. 1B). In contrast, at the three more
29 northerly seamounts, temperatures above 12°C occur down to ~ 600 m and only fall below
30 5°C at ~ 1100 m. As scleractinian CWCs are most commonly found in waters of 4-12°C
31 (Roberts et al., 2006), Coral Seamount may provide more suitable thermal conditions over a
32 wider depth range. The location of Coral Seamount south of the STF, in the transition
33 between two biogeographic provinces, could also contribute to its high diversity. In contrast,
34 at the subtropical site of Atlantis Bank no flabellids or dendrophylliids were collected. The
35 temperature profile at Atlantis Bank below 200 m is similar to Melville Bank, where
36 dendrophylliids were present, but additional factors such as low POC concentration could
37 reduce the viability of certain species at Atlantis Bank, even those known from temperate
38 locations such as *B. gigas* and *L. stokesiana* (Cairns, 1995; Cairns and Zibrowius, 1997).

39 We also find some evidence of within-species variations between the four seamounts. A
40 ‘robust’ morph of *C. diomedae*, with exert, transversally ridged and laterally protruding
41 septa was dominant at Atlantis Bank (Fig. 2A), whereas most specimens at Coral Seamount
42 had less exert septa (Fig. 2B). It is worth noting that the Atlantis specimens are dated to the
43 late Holocene, whereas all *C. diomedae* from Coral Seamount are deglacial in age. A few
44 specimens at Melville Bank and MoW Seamount share features of these two end members.
45 To some extent a similar pattern is seen in *D. dianthus*; three specimens at Atlantis Bank
46 have particularly flared septa and well-defined costae (Fig. 2C), whilst specimens to the south
47 display a smoother corallum with less exert septa (Fig. 2D). These discrepancies exist
48 between specimens of the same age at Atlantis Bank and Coral Seamount. Wide intraspecific
49 variability is a characteristic of both of these species (Addamo et al., 2015; Kitahara et al.,
50 2010), and could be due to phenotypic flexibility in different environmental conditions, or
51 genetic isolation and divergence (Miller et al., 2011). Either explanation could apply here, but
52 since the variation could best be described as a spectrum across the seamounts, it seems more

53 likely to be a response to environmental conditions such as temperature and/or food

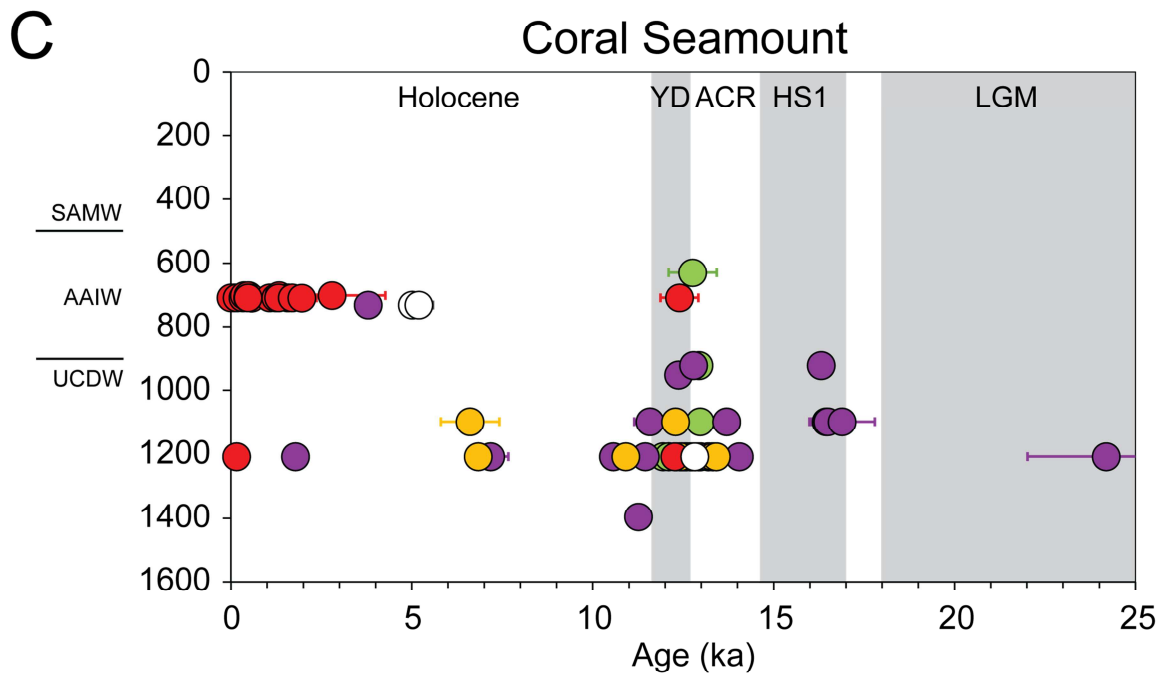
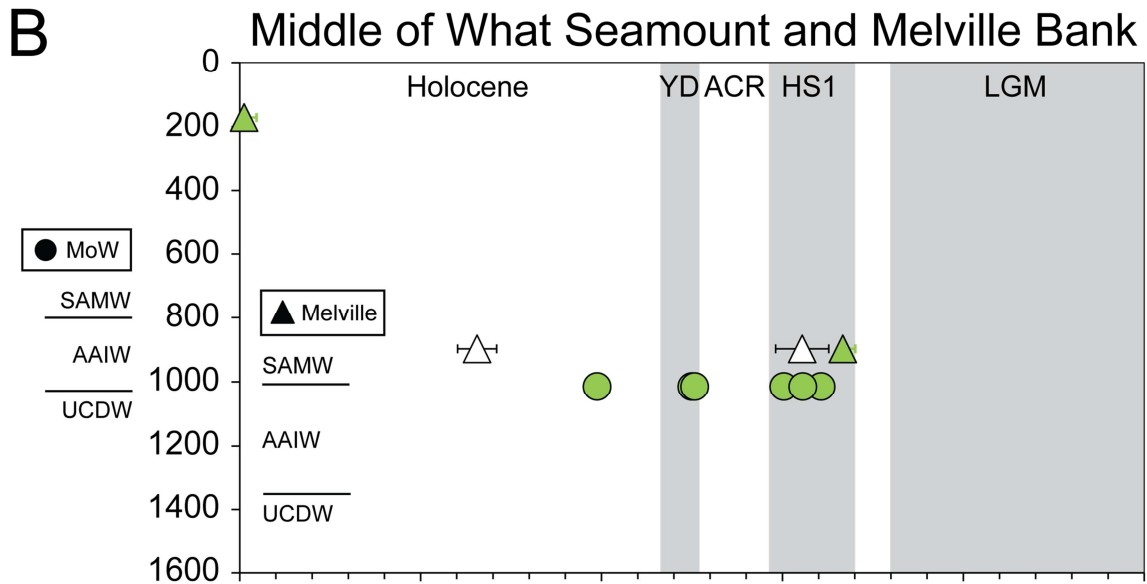
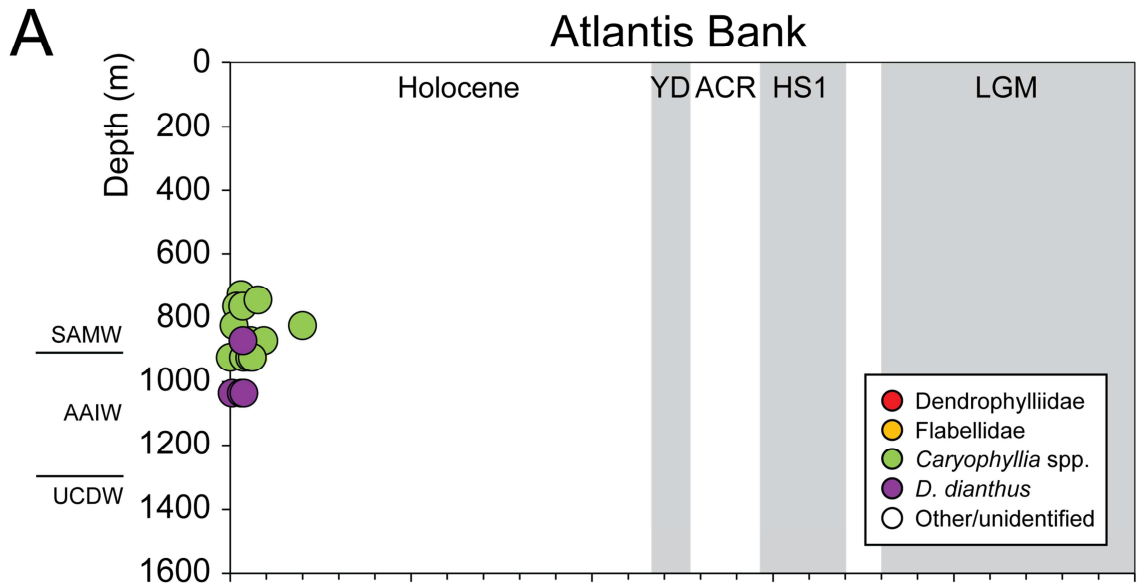
54 availability.

55 Overall, the variations in the subfossil CWC collection north and south of the STF give some
56 support to the idea of biogeographic zonation. But there are also similarities in the species
57 found, which may result from the water mass connectivity at depth. Without surveys and
58 phylogenetic analyses on modern CWCs, the importance of these two factors cannot be
59 quantified. The rarity of expeditions to the area and the disturbance of organisms and
60 substrate because of trawling in the SWIO (Rogers and Taylor, 2011) are likely to inhibit
61 these more robust investigations.

62 **4.2 Temporal shifts in CWC populations**

63 Uranium-series dating of the SWIO collection reveals variability in the distribution and
64 diversity of CWCs over the past 25,000 years. Here we discuss patterns of coral abundance in
65 relation to deglacial climate and regional oceanographic changes (Figs. 6-8).

66 Figure 6: Depths and ages of subfossil CWCs at A, Atlantis Bank; B, Melville Bank (triangles) and
67 Middle of What Seamount (dots) and C, Coral Seamount, coloured coded by taxonomic category.
68 Precise ages are given for samples which underwent isotope dilution U-series dating, and laser
69 ablation ages are used for all other samples (see Appendices 1-3). Grey and white bars indicate the
70 timings of the Holocene, Younger Dryas (YD), Antarctic Cold Reversal (ACR), Heinrich Stadial 1
71 (HS1), and the Last Glacial Maximum (LGM). The depths of boundaries between Subantarctic Mode
72 Water (SAMW), Antarctic Intermediate Water (AAIW) and Upper Circumpolar Deep Water
73 (UCDW) at each seamount are indicated by black lines.



76 One of the most notable aspects of the SWIO coral record is the absence, bar one *D. dianthus*
77 specimen, of samples dating to the LGM (Figs. 5, 6). Preservation bias cannot be ruled out,
78 though an older specimen, dated from MIS 6 (142 ± 8 ka) was found, and much older *D.*
79 *dianthus* specimens from the subpolar region have previously been recorded (Burke and
80 Robinson, 2012). It is unlikely that food supply was limiting; opal and organic carbon flux
81 increases point to higher export production in the SAZ of both the Atlantic (Martínez-García
82 et al., 2014) and Indian oceans (Dezileau et al., 2003) during the glacial. In general, coral
83 recruitment will not occur unless there is a consistent supply of larvae to the region in
84 question. Hence, the LGM absence of CWCs could indicate the existence of a barrier to
85 larval dispersal into the SWIO at that time, for example, the ACC. In the Drake Passage,
86 glacial age CWCs were found almost exclusively in the Antarctic Zone, leading Margolin et
87 al. (2014) to suggest that the Polar Front posed a barrier to larval transport further north. As
88 samples south of the Polar Front were not sampled in the SWIO, it is difficult to make direct
89 comparisons. If larval dispersal to the SWIO seamounts from south of the ACC was inhibited
90 during the glacial, a subsequent expansion of CWCs would require either a weakening of the
91 ACC flow, or a northward shift of the Southern Ocean fronts. Reconstructions of glacial flow
92 speeds suggest a similar current speed (Mastumoto et al., 2001; McCave et al., 2014) or
93 lower flow speed (Roberts et al., 2017) compared to the Holocene. In terms of frontal
94 position, it is likely that the Polar Front occupied its most northerly position during the LGM,
95 moving poleward during the early deglacial (Barker et al., 2009; De Deckker et al., 2012).
96 Therefore, evidence for the Polar Front and ACC posing a greater barrier to CWC
97 distribution in the Subantarctic and Subtropical Southern Ocean during the LGM is
98 unconvincing. If the deglacial appearance of CWCs resulted from enhanced larval transport
99 from lower latitudes, we would perhaps expect to see earlier occurrences at Atlantis Bank.
100 The circumpolar transport of the ACC, the influence of the ARC, and the overturning

101 circulation (Henry et al., 2014) could all have provided routes for widespread larval dispersal
102 throughout the glacial and in the modern day.

103 Given the likelihood of an adequate food supply and open routes for larval dispersal
104 northwards, we suggest that environmental boundary conditions limited CWC growth in the
105 SWIO during the LGM. A broad consensus exists that a large proportion of glacial CO₂ was
106 stored in the deep ocean as a result of a more effective biological pump and reduced deep
107 ocean ventilation (Kohfeld and Chase, 2017). The resulting decrease in carbonate ion
108 concentration and shoaling of the ASH (Sigman et al., 2010; Yu et al., 2010) may therefore
109 have reduced the ability of CWCs to calcify, especially in deep waters. This environment
110 may also have caused dissolution of existing subfossil CWCs, explaining the absence, bar
111 one, of corals dating to earlier periods of more favourable climate conditions. Trace metal
112 evidence also suggests intermediate waters were depleted in dissolved oxygen (Durand et al.,
113 2018; Jaccard et al., 2016), likely resulting from stratification and increased isolation from
114 the atmosphere (Burke et al., 2015). In addition, temperatures in intermediate waters are
115 estimated to have been 3-5°C lower at this time compared to the Holocene, and deep waters
116 ~3°C cooler than the deglacial maxima (Fig. 7E; Elmore et al., 2015; Roberts et al., 2016).
117 We therefore suggest that a shoaled ASH and cool, deoxygenated intermediate waters
118 contributed to unfavourable conditions for CWC growth during the glacial, outcompeting any
119 possible benefits of enhanced food supply. Glacial subfossil coral abundance is also low
120 south of Tasmania (Fig. 7B; Thiagarajan et al., 2013) and in the subantarctic Drake Passage
121 (Fig. 7C; Margolin et al., 2014), supporting a consistent circumpolar response of CWCs to
122 the glacial boundary conditions.

123 *4.2.2 The early deglacial, Heinrich Stadial 1*

124 The early deglacial appearance of CWCs at the three seamounts south of the STF (Coral,
125 Melville and MoW; Fig. 6) is concurrent with the onset of Antarctic warming and Heinrich

126 Stadal 1 (HS1; 18-14.7 ka; Fig. 7A) ~18 ka ago. During this time interval, release of a deep
127 inorganic carbon pool through processes in the Southern Ocean is thought to have contributed
128 to the atmospheric CO₂ rise (Marcott et al., 2014). Increases in benthic $\delta^{13}\text{C}$ (Ninnemann and
129 Charles, 2002; Roberts et al., 2016), reductions in deep water ventilation age (Burke and
130 Robinson, 2012; Skinner et al., 2010), and increases in abyssal carbonate ion concentrations
131 (Yu et al., 2010) all support the deep ocean ventilation hypothesis. These processes may have
132 resulted in a deepening of the ASH and improved conditions for CWC calcification.
133 However, such changes in the deep and abyssal oceans may not have reached depths less than
134 1400 m at which CWCs were found; on the contrary, depletions in intermediate water
135 radiocarbon have been reported (Bryan et al., 2010; Romahn et al., 2014), likely reflecting
136 transient transport of the deep stored carbon into shallower levels before its release to the
137 atmosphere.

138 During HS1, increased oxygenation is recorded in the deep Southern Ocean (Jaccard et al.,
139 2016) and the intermediate northern Indian Ocean (Jaccard and Galbraith, 2012), which
140 would have contributed to improving conditions for CWC growth. It is also possible that
141 coral population growth was boosted by increased food supply in the form of sinking
142 particulate organic matter, given the increase in opal flux in the Pacific and Atlantic sectors
143 of the Southern Ocean at this time (Anderson et al., 2009; Fig. 7D). We therefore suggest that
144 the simultaneous appearance of subfossil corals in the SWIO, Tasmania (Thiagarajan et al.,
145 2013), and the subantarctic Drake Passage (Margolin et al., 2014) during HS1 could have
146 been facilitated by increasing oxygen concentrations and food supply, but was still limited by
147 carbonate chemistry at mid-depths, particularly in the Indian and Pacific sectors of the
148 Southern Ocean. Cold-water coral growth also seems to have been enhanced off the coast of
149 Brazil during this time, potentially as a result of increased upwelling and food supply
150 (Mangini et al., 2010).

152 The greatest abundance of subfossil CWCs in the SWIO occurs in the late deglacial (33
153 specimens; Figs. 6, 7A), predominantly within the Younger Dryas (YD), between 13.5 and
154 11.5 ka. During this period, Coral Seamount supported a diverse community of at least seven
155 solitary scleractinian species including *C. diomedea*, *F. flexuosum* and *J. antarctica*.
156 Notably, this peak in abundance is located at UCDW depths (~ 900-1400 m at Coral
157 Seamount), with only four specimens found at modern-day AAIW depths. Late deglacial
158 abundance peaks also occur at modern UCDW depths in the Tasmanian (Fig. 7B) and Drake
159 Passage collections (Fig. 7C).

160 As AAIW depths appear to be preferable for CWCs in the late Holocene, it is tempting to
161 explain their presence deeper in the water column during the deglaciation by a deepening of
162 AAIW and displacement of the lower-oxygen UCDW. Water mass boundaries will have
163 occupied deeper positions in the water column as a result of lower sea level; however this
164 effect can only account for ~60 m displacement between the YD and Holocene, rather than
165 the observed 200 – 500 m depth shift observed at Coral Seamount. Because of the sloping
166 isopycnals in this region (Fig. 1), a more southerly position of the SAF would effectively
167 deepen AAIW at the SWIO and seamounts and around Tasmania. However, reconstructions
168 suggest the SAF occupied a similar position to the present day during the late deglacial (De
169 Deckker et al., 2012; Roberts et al., 2017). A deepening of AAIW would also not explain the
170 relative lack of corals from < 900 m. Hence, we consider other possible controls on the CWC
171 distribution.

172 Oxygen concentrations below ~145 $\mu\text{mol/kg}$ have been shown to limit respiration of certain
173 *D. pertusum* (= *L. pertusa*) specimens in laboratory experiments (Dodds et al., 2007). An
174 early- to mid-Holocene decline of CWC populations in the Mediterranean has been linked to
175 a fall in oxygenation below ~180 $\mu\text{mol/kg}$ (Fink et al., 2012), and low oxygen also appears to

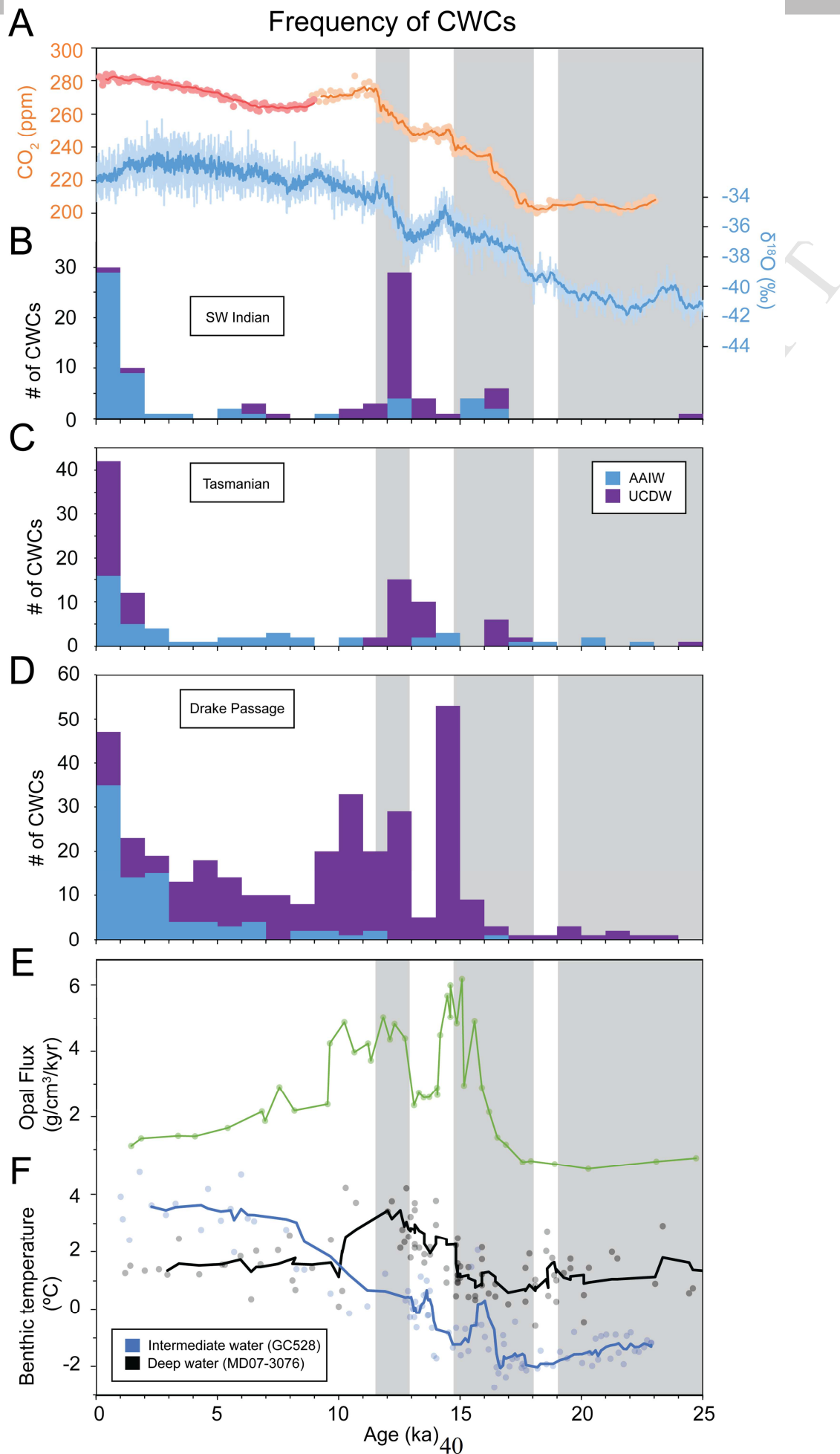
176 affect the distribution of CWCs in the late Holocene south of Tasmania (Thiagarajan et al.,
177 2013). Elevated oxygen concentrations recorded in the intermediate northern Indian Ocean
178 (Jaccard and Galbraith, 2012) and the deep Southern Ocean (Jaccard et al., 2016) during the
179 period of relative CWC abundance in the SWIO, suggest a plausible role for oxygenation.
180 Intermediate water pH in the Drake Passage also peaked during this time (Rae et al., 2018).
181 Although these ocean chemistry reconstructions cover density intervals below the corals in
182 this collection, chemical changes could feasibly have been communicated to UCDW depths.
183 Increased food availability is also an important driver of CWC fitness (Naumann et al.,
184 2011), and for cold water corals this consists of particulate organic carbon and
185 microorganisms (Roberts et al., 2009). There is clear evidence for higher export production in
186 the Antarctic Zone of the Atlantic Southern Ocean at 13-11.5 ka, coeval with the CWC
187 abundance peak (Anderson et al., 2009; Fig. 7D). Enhanced export production could have
188 resulted in higher POC concentrations at depth, supplying CWCs with nutrition in the SAZ.
189 However, the most likely path for northward transport of this food supply would be in surface
190 currents and AAIW via Ekman pumping (Marshall and Speer, 2012). In the SWIO, UCDW
191 flows northward above 1500 m (McCave et al., 2005), so could also have advected POC
192 northwards towards Coral Seamount, but it seems unlikely that it would have been the main
193 conduit. Productivity peaks and an associated increase in food availability may explain the
194 overall increase in abundance of CWCs during the late deglacial period, but do not explain
195 the apparent preference for UCDW depths.

196 Global scale modelling of CWC distribution shows a strong correlation with temperature
197 (Davies and Guinotte, 2011), and although a lower limit has not been tested in laboratory
198 experiments (to our knowledge), CWCs are rarely found below temperatures of 1°C (Stanley
199 and Cairns, 1988). *Desmophyllum dianthus* has been found in waters as cold as 1°C in the
200 Drake Passage (Margolin et al., 2014), and in the late Holocene SWIO we find specimens at
201 depths corresponding to modern temperatures of between ~16°C and 3°C. In the subantarctic

202 South Atlantic, Mg/Ca-derived temperature reconstructions suggest that intermediate waters
203 were colder than deep waters for much of the deglacial interval, initially at -1 to -2°C and
204 remaining below 1°C until the early Holocene (Roberts et al., 2016; Fig.7E). Deep waters
205 were warmer at around 0-2 °C during the early deglacial and reached a peak of 4°C between
206 13 and 11ka, with a stable vertical density stratification being conserved because of higher
207 salinities at depth (Adkins et al., 2002; Roberts et al., 2016). Therefore, we propose that low
208 temperatures may have been an important factor in the relative paucity of CWCs from AAIW
209 depths during the deglacial. In addition, we note that deep waters in the Indian, Pacific, and
210 Atlantic oceans reached a peak in carbonate ion concentration between 15 and 10 ka (Yu et
211 al., 2010). Such globally enhanced carbonate ion concentrations would have deepened the
212 ASH, and possibly enabled the expansion of CWCs into CDW, which by that time had
213 reached a warmer and more optimal temperature.

214 In summary, we propose that increased oxygenation, a deepened ASH, warmer temperatures,
215 and a peak in regional food supply created suitable conditions for CWC growth in UCDW
216 depths during the YD. In contrast, CWCs may have been unable to survive at AAIW depths
217 until the salinity-controlled stratification broke down and temperatures increased in the
218 Holocene.

219 Figure 7: Number of cold-water corals (CWCs) per 1000-year age bin at three Southern Ocean
220 locations, coded by water mass, with Antarctic Intermediate Water (AAIW) in blue and Upper
221 Circumpolar Deep Water (UCDW) in purple. Precise ages are given for samples which underwent
222 isotope dilution U-series dating, and laser ablation ages are used for all other samples (see Appendices
223 1-3). A, SW Indian CWCs (this study), overlain with the West Antarctic Ice Sheet (WAIS) Divide
224 Core $\delta^{18}\text{O}$ record and 11-point moving average (WAIS Divide Project Members, 2015), and
225 composite CO_2 record with 5-point moving averages from WDC (orange, Marcott et al., 2014) and
226 EPICA (red, Monnin et al., 2001). B, Tasmanian *D. dianthus* abundances (Thiagarajan et al, 2013),
227 assigned to water mass following Hines et al. (2015; AAIW 500-1500m). C, Drake Passage *D.*
228 *dianthus* abundances, using water mass designations from Margolin et al. (2014). D, Opal flux record
229 from South Atlantic core TN057-13-4PC (53.1728°S, 5.1275°E, 2848m; Anderson et al., 2009). E,
230 Mg/Ca-derived benthic temperatures for intermediate (GC528, 598m; blue) and deep waters (MD07-
231 3076, 3770m; black) from the subantarctic South Atlantic (Roberts et al., 2016).



234 4.2.4 *The Holocene*

235 Specimens from the early- to mid-Holocene are notably scarce in the SWIO collection, with
236 only seven specimens dating to between 5 and 10 ka, all collected from south of the STF
237 (Figs. 5, 6A). Those that were found are poorly preserved (Fig. 4), possibly indicating greater
238 susceptibility to degradation. During this time interval, deep water carbonate ion
239 concentrations reached their lowest values (Yu et al., 2010). It is possible that a shoaled ASH
240 reduced the suitability of UCDW, whilst the temperature of AAIW was still sub-optimal for
241 coral growth (Fig. 7E; Roberts et al., 2016). Corals are present throughout this period in the
242 Tasmanian and Drake Passage collections (Fig. 7B, C), but at much lower abundances than
243 during the ACR (Margolin et al., 2014; Thiagarajan et al., 2013).

244 After this decrease in abundance, the number of CWC specimens increases at Coral and
245 Atlantis (Fig. 6). Late Holocene CWC specimens are found at shallower depths compared to
246 the deglacial period, with 95 % of CWC dated to < 6 ka being found in SAMW or AAIW
247 (Fig. 7A). Only two specimens dated to < 6 ka are found below 750 m at Coral Seamount,
248 within UCDW depths, and no live corals were seen below 700 m during ROV surveys
249 (Rogers and Taylor, 2011). In the southeast Pacific (Cape Horn) and Drake Passage
250 (Burdwood Bank), Late Holocene corals are also more common above 1000 m (Margolin et
251 al., 2014; Fig. 7C). South of Tasmania, the CWCs undergo a depth expansion from 2000 to
252 2400 m in CDW depths, with abundant corals also at shallower AAIW depths, but with a
253 'hiatus' at depths of 1500-1800 m influenced by lower dissolved oxygen values (170-180
254 $\mu\text{mol/kg}$; (Thiagarajan et al., 2013).

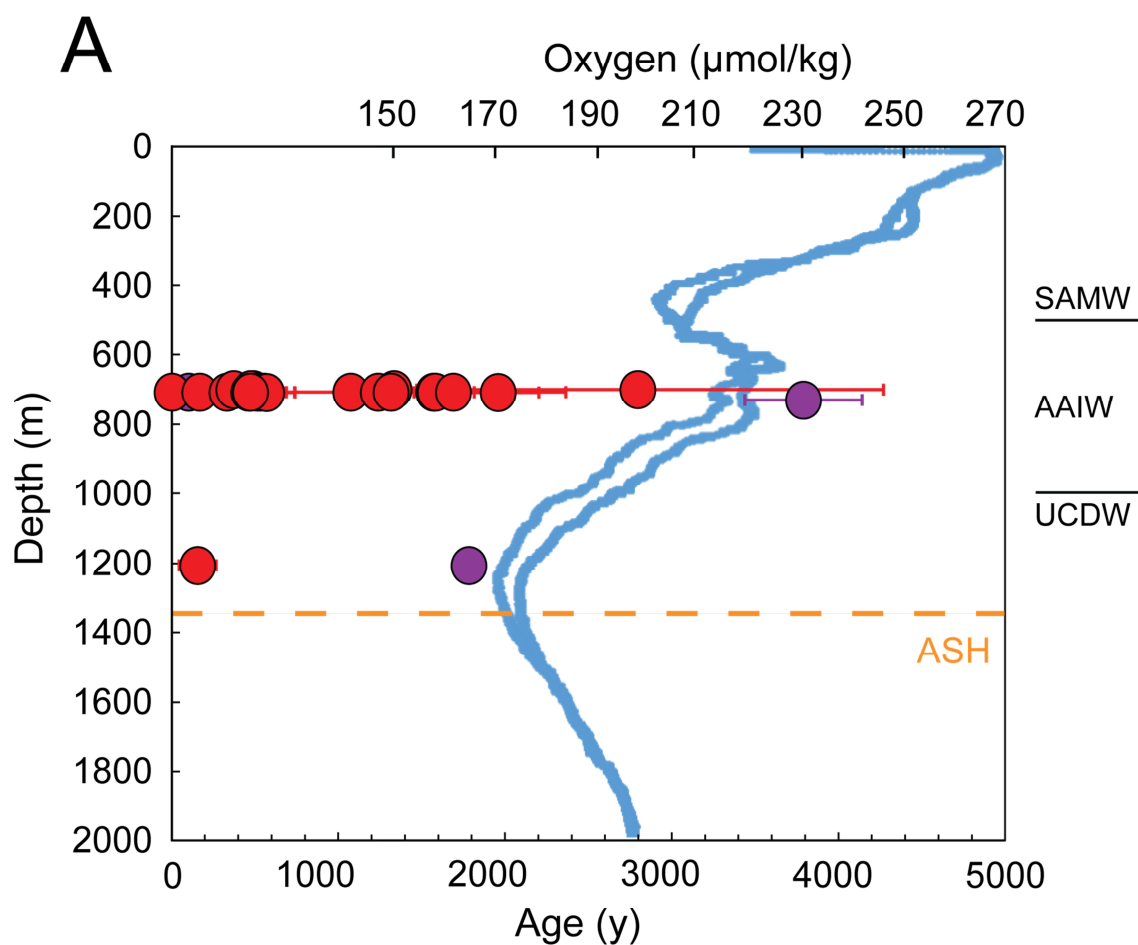
255 In the modern subantarctic SWIO, 900-1000 m marks the upper boundary of UCDW, a water
256 mass which brings in old, nutrient-rich deep waters from the northern Indian Ocean and
257 which is associated with a similar dissolved oxygen minimum (< 180 $\mu\text{mol O}_2/\text{kg}$ from 1000

258 – 1500 m; Figs. 1B, 7) to the Tasmanian coral hiatus (Thiagarajan et al., 2013). The depth of
259 the ASH, controlled mainly by temperature and pressure, is also approximately coincident
260 with UCDW in the region of Coral Seamount (~ 1400 m; Sabine et al., 2002; Fig. 8). Because
261 sampling did not take place below the ASH or oxygen minimum, it is difficult to evaluate
262 their relative influence. However, the coincidence of most late Holocene CWCs between 600
263 and 800 m with the oxygen peak within AAIW (~220 $\mu\text{mol/kg}$) is striking.

264 The absence of CWCs from Atlantis Bank before the late Holocene (Fig. 6A) is difficult to
265 explain in terms of any of the above discussed environmental factors, and may instead be an
266 artefact of the limited depth survey performed there. Today, surface waters at Atlantis Bank
267 have the lowest chlorophyll fluorescence of the four seamounts (Djurhuus et al., 2017b),
268 indicating low productivity and a limited food source, although modern corals there may
269 benefit from organic matter export via SAMW. If anything, food supply at Atlantis Bank is
270 likely to have been higher in the past as a result of increased iron fertilisation (Kohfeld et al.,
271 2005) and a northward-shifted STF (De Deckker et al., 2012; Sikes et al., 2009), making food
272 supply an unlikely factor in controlling their absence. Similarly, temperatures were likely no
273 warmer and oxygen concentrations similar throughout the Holocene at these depths.

274 However, it could perhaps be the case that favourable calcification conditions arose only in
275 the late Holocene, because the ASH shoals to the north in the modern day SWIO (Sabine et
276 al., 2002), making this location particularly sensitive to changes in ocean carbonate
277 chemistry.

278 Figure 8: Depths and ages (lower axis) of Late Holocene corals at Coral Seamount, colour coded by
279 taxonomic grouping where red dots are Dendrophylliidae and purple dots are *Desmophyllum dianthus*.
280 Precise ages are given for samples which underwent isotope dilution U-series dating, and laser
281 ablation ages are used for all other samples (see Appendices 1-3). Blue curves show seawater oxygen
282 concentration from CTD data at Coral Seamount (upper axis) and the approximate depth of the
283 aragonite saturation horizon (ASH; Sabine et al., 2002) is indicated in orange. Modern day boundaries
284 between Subantarctic Mode Water (SAMW), Antarctic Intermediate Water (AAIW) and Upper
285 Circumpolar Deep Water (UCDW) are indicated with black lines.



286

287

289 The species assemblage of subfossil scleractinian corals recovered from SWIO seamounts
290 indicates influences from the Indian, Pacific, and Antarctic biogeographic zones. Particular
291 diversity and abundance of CWCs at Coral Seamount may be a result of its location in the
292 SAZ, between the Antarctic and Indian biogeographic zones, and higher food availability.
293 We also find indications of biogeographic controls on morphology across the seamount
294 transect, with a more robust *D. dianthus* and *C. diomedea* morphology occurring more
295 commonly north of the STF, compared to specimens from intermediate and deep waters in
296 the SAZ.

297 Striking similarities in the temporal distribution of CWCs from the SWIO with other
298 Southern Ocean CWC collections hint at widespread impacts on coral habitats from deglacial
299 changes in ocean stratification and biogeochemistry. As observed elsewhere in the subpolar
300 Southern Ocean, solitary coral growth seems to have been limited during the LGM.
301 Unfavourable carbonate, temperature, and oxygen conditions may have outweighed higher
302 productivity in the SAZ. Although CWCs begin to appear during HS1, we argue that
303 carbonate and oxygen conditions did not become optimal until the late deglacial (14 -11.5
304 ka), when a peak in abundance is seen in solitary CWC records from the SWIO, Tasmania,
305 and the Drake Passage. This abundance peak is coincident with increased productivity in the
306 Antarctic Zone, which could have provided enhanced supply of POC to the SAZ sites via
307 advection. Water temperatures within AAIW may have been below the habitable range, a
308 possible explanation for the relative lack of solitary CWCs at intermediate depths at this time.
309 In contrast, warmer temperatures within UCDW, combined with greater oxygenation, higher
310 deep-water carbonate ion concentrations and a deeper ASH than during the LGM, could have
311 facilitated colonisation at UCDW depths.

312 In the late Holocene SAZ, the mid-depth oxygen minimum associated with the inflow of old
313 deep waters from the Indian and Pacific Oceans appears to have been a less favourable
314 habitat for solitary CWCs in the SWIO and Tasmania than well-oxygenated AAIW depths.
315 This observation suggests that their survival here requires higher oxygen concentrations than
316 cold-water coral reefs elsewhere. Future investigations on larger numbers of CWCs, collected
317 in a systematic survey of this region, combined with a greater understanding of the responses
318 of solitary CWC to environmental conditions, would likely provide stronger constraints on
319 the patterns we describe, and on future responses of CWCs to environmental change.

320 **Acknowledgements**

321 The JC066 RRS James Cook expedition was supported by the Global Environment Facility
322 Grant through UNDP Project ID GEF3138/PIMS3657, the IUCN Seamounts Project FFEM-
323 SWIO-P00917, and NERC Grant NE/F005504/1 Benthic Biodiversity of Seamounts in the
324 Southwest Indian Ocean. We thank the science teams and crews of expedition JC066 for
325 collecting the coral samples, and Anni Djurhuus for sharing cruise data. We acknowledge
326 NERC funding to NP through the Science and Solutions for a Changing Planet DTP
327 (NE/L002515/1), TvdF and DJW (NE/N001141/1), SHL (NERC fellowship, NE/
328 P018181/1), NS (NERC NE/R011044/1) and LR (NE/N003861/1). SHL also acknowledges
329 support from a Leverhulme Trust fellowship (ECF-2014-615), and LR from the European
330 Research Council (278705). We are grateful for technical and lab support from Katharina
331 Kreissig, Barry Coles and Carolyn Taylor, and thank Ken Johnson for supervision at the
332 Natural History Museum. We also thank Igor Belkin for editorial handling and Andres
333 Rüggeberg, Jean-Carlos Montero-Serrano and two anonymous reviewers for constructive
334 comments on the manuscript.

335 **References**

- 336 Addamo, A.M., Martínez-Baraldés, I., Vertino, A., López-González, P.J., Taviani, M.,
337 Machordom, A., 2015. Morphological polymorphism of *Desmophyllum dianthus*
338 (Anthozoa: Hexacorallia) over a wide ecological and biogeographic range: Stability in
339 deep habitats? *Zool. Anz.* 259, 113–130. <https://doi.org/10.1016/j.jcz.2015.10.004>
- 340 Adkins, J.F., McIntyre, K., Schrag, D.P., 2002. The salinity, temperature, and $\delta^{18}\text{O}$ of the
341 glacial deep ocean. *Science* 298, 1769–1773.
- 342 Alcock, A., 1902. Report on the deep-sea Madreporaria of the Siboga-Expedition. E. J. Brill,
343 Leiden.
- 344 Anderson, B.E., Ali, S., Bradtmiller, L.I., Nielsen, S.H.H., Fleisher, M.Q., Anderson, B.E.,
345 Burckle, L.H., 2009. Wind-driven upwelling in the Southern Ocean and the deglacial
346 rise in atmospheric CO_2 . *Science* 323, 1443–1448.
- 347 Baco, A.R., Morgan, N., Roark, E.B., Silva, M., Shamberger, K.E.F., Miller, K., 2017.
348 Defying dissolution: Discovery of deep-sea scleractinian coral reefs in the North Pacific.
349 *Sci. Rep.* 7, 5436. <https://doi.org/10.1038/s41598-017-05492-w>
- 350 Bard, E., Rickaby, R.E.M., 2009. Migration of the subtropical front as a modulator of glacial
351 climate. *Nature* 460, 380–383. <https://doi.org/10.1038/nature08189>
- 352 Barker, S., Diz, P., Vautravers, M.J., Pike, J., Knorr, G., Hall, I.R., Broecker, W.S., Diz, P.,
353 Knorr, G., 2009. Interhemispheric Atlantic seesaw response during the last deglaciation.
354 *Nature* 457, 1097–1102. <https://doi.org/10.1038/nature07770>
- 355 Beal, L.M., De Ruijter, W.P.M., Biastoch, A., Zahn, R., Cronin, M., Hermes, J., Lutjeharms,
356 J., Quartly, G., Tozuka, T., Baker-Yeboah, S., Bornman, T., Cipollini, P., Dijkstra, H.,
357 Hall, I., Park, W., Peeters, F., Penven, P., Ridderinkhof, H., Zinke, J., 2011. On the role

358 of the Agulhas system in ocean circulation and climate. *Nature* 472, 429–436.
359 <https://doi.org/10.1038/nature09983>

360 Belkin, I.M., Gordon, A.L., 1996. Southern Ocean fronts from the Greenwich meridian to
361 Tasmania. *J. Geophys. Res.* 101, 3675–3696. <https://doi.org/10.1029/95JC02750>

362 Bourne, G.C., 1905. Report on the solitary corals collected by Professor Herdman, at Ceylon,
363 in 1902. Rep. to Gov. Ceylon Pearl Oyster Fish. Gulf Manaar 4, 187–211.

364 Bryan, S.P., Marchitto, T.M., Lehman, S.J., 2010. The release of ^{14}C -depleted carbon from
365 the deep ocean during the last deglaciation: Evidence from the Arabian Sea. *Earth*
366 *Planet. Sci. Lett.* 298, 244–254. <https://doi.org/10.1016/j.epsl.2010.08.025>

367 Burke, A., Robinson, L.F., 2012. The Southern Ocean's role in carbon exchange during the
368 last deglaciation. *Science* 335, 557–561. <https://doi.org/10.1126/science.1208163>

369 Burke, A., Robinson, L.F., McNichol, A.P., Jenkins, W.J., Scanlon, K.M., Gerlach, D.S.,
370 2010. Reconnaissance dating: A new radiocarbon method applied to assessing the
371 temporal distribution of Southern Ocean deep-sea corals. *Deep. Res. Part I Oceanogr.*
372 *Res. Pap.* 57, 1510–1520. <https://doi.org/10.1016/j.dsr.2010.07.010>

373 Burke, A., Stewart, A.L., Adkins, J.F., Ferrari, R., Jansen, M.F., Thompson, A.F., 2015. The
374 glacial mid-depth radiocarbon bulge and its implications for the overturning circulation.
375 *Paleoceanography* 1021–1039. <https://doi.org/10.1002/2015PA002778>. Received

376 Büscher, J. V., Form, A.U., Riebesell, U., 2017. Interactive effects of ocean acidification and
377 warming on growth, fitness and survival of the cold-water coral *Lophelia pertusa* under
378 different food availabilities. *Front. Mar. Sci.* 4, 1–14.
379 <https://doi.org/10.3389/fmars.2017.00101>

380 Cairns, S.D., 2007. Deep water corals : an overview with special reference to diversity and

- 381 distribution of deep-water scleractinian corals. *Bull. Mar. Sci.* 81, 311–322.
- 382 Cairns, S.D., 2000. A revision of the shallow-water azooxanthellate Scleractinia of the
383 western Atlantic. *Stud. Nat. Hist. Carribean Reg.* 75, 1–215.
- 384 Cairns, S.D., 1995. The marine fauna of New Zealand: Scleractinia (Cnidaria Anthozoa).
385 New Zeal. Oceanogr. Inst. Mem. 103, 210.
386 <https://doi.org/10.1017/CBO9781107415324.004>
- 387 Cairns, S.D., 1982. Antarctic and Subantarctic Scleractinia. *Biol. Antarct. Seas XI Antarct.*
388 *Res. Ser.* 34, 1–74.
- 389 Cairns, S.D., Keller, N.B., 1993. New taxa distributional records of azooxanthellate
390 Scleractinia (Cnidaria, Anthozoa) from the tropical southwest Indian Ocean, with
391 comments on their zoogeography and ecology. *Ann. South African Museum* 103, 213–
392 292.
- 393 Cairns, S.D., Polonio, V., 2013. New records of deep-water Scleractinia off Argentina and
394 the Falkland Islands. *Zootaxa* 3691, 58–86. <https://doi.org/10.11646/zootaxa.3691.1.2>
- 395 Cairns, S.D., Zibrowius, H., 1997. Cnidaria Anthozoa : azooxanthellate Scleractinia from the
396 Philippine and Indonesian regions. *Mem. du Museum Natl. d’Histoire Nat.* 172, 27–243.
- 397 Chen, T., Robinson, L.F., Burke, A., Southon, J., Spooner, P., Morris, P.J., Ng, H.C., 2015a.
398 Synchronous centennial abrupt events in the ocean and atmosphere during the last
399 deglaciation. *Science* 349, 1537–1542. <https://doi.org/10.1126/science.aac6159>
- 400 Chen, T., Robinson, L.F., Burke, A., Southon, J., Spooner, P., Morris, P.J., Ng, H.C., Morris,
401 P.J., Burke, A., Southon, J., Robinson, L.F., Spooner, P., 2015b. Synchronous centennial
402 abrupt events in the ocean and atmosphere during the last deglaciation. *Science* (80-.).
403 349, 1537–1541. <https://doi.org/10.1126/science.aac6159>

404 Cheng, H., Adkins, J., Edwards, R.L., Boyle, E.A., 2000a. U-Th dating of deep-sea corals.
405 *Geochim. Cosmochim. Acta* 64, 2401–2416.

406 Cheng, H., Adkins, J., Edwards, R.L.L., Boyle, E.A., 2000b. U-Th dating of deep-sea corals.
407 *Geochim. Cosmochim. Acta* 64, 2401–2416. [https://doi.org/10.1016/S0016-](https://doi.org/10.1016/S0016-7037(99)00422-6)
408 [7037\(99\)00422-6](https://doi.org/10.1016/S0016-7037(99)00422-6)

409 Crocket, K.C., Lambelet, M., van de Flierdt, T., Rehkämper, M., Robinson, L.F., 2014.
410 Measurement of fossil deep-sea coral Nd isotopic compositions and concentrations by
411 TIMS as NdO⁺, with evaluation of cleaning protocols. *Chem. Geol.* 374–375, 128–140.
412 <https://doi.org/10.1016/j.chemgeo.2014.03.011>

413 Dana, J.D., 1846. *Structure and Classification of Zoophytes*. Lea and Blanchard,
414 Philadelphia.

415 Davies, A.J., Guinotte, J.M., 2011. Global habitat suitability for framework-forming cold-
416 water corals. *PLoS One* 6, e18483. <https://doi.org/10.1371/journal.pone.0018483>

417 De Deckker, P., Moros, M., Perner, K., Jansen, E., 2012. Influence of the tropics and
418 southern westerlies on glacial interhemispheric asymmetry. *Nat. Geosci.* 5, 266–269.
419 <https://doi.org/10.1038/ngeo1431>

420 de Pourtalès, L.F., 1878. Reports on the results of dredging, under the supervision of
421 Alexander Agassiz, in the Gulf of Mexico, by the United States Coast Survey Steamer
422 “Blake”: Corals. *Bull. Museum Comp. Zool.* 5, 197–212.

423 de Pourtalès, L.F., 1871. Deep-sea corals, in: *Illustrated Catalogue of the Museum of*
424 *Comparative Zoology*. p. 93.

425 Dezileau, L., Reyss, J.L., Lemoine, F., 2003. Late Quaternary changes in biogenic opal fluxes
426 in the Southern Indian Ocean. *Mar. Geol.* 202, 143–158. <https://doi.org/10.1016/S0025->

- 428 Djurhuus, A., Boersch-Supan, P.H., Mikalsen, S.O., Rogers, A.D., 2017a. Microbe
429 biogeography tracks water masses in a dynamic oceanic frontal system. *R. Soc. Open*
430 *Sci.* 4, 170033. <https://doi.org/10.1098/rsos.170033>
- 431 Djurhuus, A., Read, J.F., Rogers, A. D., 2017b. The spatial distribution of particulate organic
432 carbon and microorganisms on seamounts of the South West Indian Ridge. *Deep. Res.*
433 *Part II Top. Stud. Oceanogr.* 136, 73–84. <https://doi.org/10.1016/j.dsr2.2015.11.015>
- 434 Dodds, L.A., Roberts, J.M., Taylor, A.C., Marubini, F., 2007. Metabolic tolerance of the
435 cold-water coral *Lophelia pertusa* (Scleractinia) to temperature and dissolved oxygen
436 change. *J. Exp. Mar. Bio. Ecol.* 349, 205–214.
437 <https://doi.org/10.1016/j.jembe.2007.05.013>
- 438 Douville, E., Sallé, E., Frank, N., Eisele, M., Pons-Branchu, E., Ayrault, S., 2010. Rapid and
439 accurate U-Th dating of ancient carbonates using inductively coupled plasma-
440 quadrupole mass spectrometry. *Chem. Geol.* 272, 1–11.
441 <https://doi.org/10.1016/j.chemgeo.2010.01.007>
- 442 Dueñas, L.F., Tracey, D.M., Crawford, A.J., Wilke, T., Alderslade, P., Sánchez, J.A., 2016.
443 The Antarctic Circumpolar Current as a diversification trigger for deep-sea octocorals.
444 *BMC Evol. Biol.* 16, 2. <https://doi.org/10.1186/s12862-015-0574-z>
- 445 Duineveld, G.C.A., Lavaleye, M.S.S., Bergman, M.J.N., De Stigter, H., Mienis, F., 2007.
446 Trophic structure of a cold-water coral mound community (Rockall Bank, NE Atlantic)
447 in relation to the near-bottom particle supply and current regime. *Bull. Mar. Sci.* 81,
448 449–467.
- 449 Dullo, W.C., Flögel, S., Rüggeberg, A., 2008. Cold-water coral growth in relation to the
450 hydrography of the Celtic and Nordic European continental margin. *Mar. Ecol. Prog.*

452 Duncan, P.M., 1873. A description of the Madreporaria dredged up during the expeditions of
453 H.M.S. “Porcupine” in 1869 and 1870. Part I. Trans. Zool. Soc. London 8, 303–344.
454 <https://doi.org/10.1111/j.1096-3642.1873.tb00560.x>

455 Durand, A., Chase, Z., Noble, T.L., Bostock, H., Jaccard, S.L., Townsend, A.T., Bindoff,
456 N.L., Neil, H., Jacobsen, G., 2018. Reduced oxygenation at intermediate depths of the
457 southwest Pacific during the last glacial maximum. Earth Planet. Sci. Lett. 491, 48–57.
458 <https://doi.org/10.1016/j.epsl.2018.03.036>

459 Elmore, A.C., McClymont, E.L., Elderfield, H., Kender, S., Cook, M.R., Leng, M.J.,
460 Greaves, M., Misra, S., 2015. Antarctic Intermediate Water properties since 400 ka
461 recorded in infaunal (*Uvigerina peregrina*) and epifaunal (*Planulina wuellerstorfi*)
462 benthic foraminifera. Earth Planet. Sci. Lett. 428, 193–203.
463 <https://doi.org/10.1016/j.epsl.2015.07.013>

464 Esper, E.J.C., 1794. Die Pflanzenthiere in Abbildungen nach der Natur mit Farben erleuchtet
465 nebst Beschreibungen. Raspeschen Buchhandlung, Nürnberg.

466 Ferrari, R., Jansen, M.F., Adkins, J.F., Burke, A., Stewart, A.L., Thompson, A.F., Ferrari, R.,
467 Jansen, M.F., Adkins, J.F., Burke, A., Thompson, A.F., 2014. Antarctic sea ice control
468 on ocean circulation in present and glacial climates. Proc. Natl. Acad. Sci. 111, 8753–
469 8758. <https://doi.org/10.1073/pnas.1323922111>

470 Fink, H.G., Wienberg, C., Hebbeln, D., McGregor, H. V., Schmiedl, G., Taviani, M.,
471 Freiwald, A., 2012. Oxygen control on Holocene cold-water coral development in the
472 eastern Mediterranean Sea. Deep. Res. Part I Oceanogr. Res. Pap. 62, 89–96.
473 <https://doi.org/10.1016/j.dsr.2011.12.013>

474 Franzese, A.M., Hemming, S.R., Goldstein, S.L., Anderson, R.F., 2006. Reduced Agulhas

475 Leakage during the Last Glacial Maximum inferred from an integrated provenance and
476 flux study. *Earth Planet. Sci. Lett.* 250, 72–88.
477 <https://doi.org/10.1016/j.epsl.2006.07.002>

478 Gori, A., Ferrier-Pagès, C., Hennige, S.J., Murray, F., Rottier, C., Wicks, L.C., Roberts, J.M.,
479 2016. Physiological response of the cold-water coral *Desmophyllum dianthus* to thermal
480 stress and ocean acidification. *PeerJ* 2016, e1606. <https://doi.org/10.7717/peerj.1606>

481 Gravier, C., 1914. Sur une espèce nouvelle de Madréporaire (*Desmophyllum antarcticum*).
482 *Bull. Muséum Hist. Nat. Paris* 20, 236–238.

483 Gray, J.E., 1847. An outline of an arrangement of stony corals. *Ann. Mag. Nat. Hist. Ser. 1*
484 19, 120–128.

485 Guinotte, J.M., Orr, J., Cairns, S., Freiwald, A., Morgan, L., George, R., 2006. Will human-
486 induced changes in seawater chemistry alter the distribution of deep-sea scleractinian
487 corals? *Front. Ecol. Environ.* 4, 141–146. [https://doi.org/10.1890/1540-](https://doi.org/10.1890/1540-9295(2006)004[0141:WHCISC]2.0.CO;2)
488 [9295\(2006\)004\[0141:WHCISC\]2.0.CO;2](https://doi.org/10.1890/1540-9295(2006)004[0141:WHCISC]2.0.CO;2)

489 Henry, L.A., Frank, N., Hebbeln, D., Wienberg, C., Robinson, L.F., van de Flierdt, T., Dahl,
490 M., Douarin, M., Morrison, C.L., Correa, M.L., Rogers, A.D., Ruckelshausen, M.,
491 Roberts, J.M., 2014. Global ocean conveyor lowers extinction risk in the deep sea. *Deep.*
492 *Res. Part I Oceanogr. Res. Pap.* 88, 8–16. <https://doi.org/10.1016/j.dsr.2014.03.004>

493 Hines, S.K. V, Southon, J.R., Adkins, J.F., 2015. A high-resolution record of Southern Ocean
494 intermediate water radiocarbon over the past 30,000 years. *Earth Planet. Sci. Lett.* 432,
495 46–58. <https://doi.org/10.1016/j.epsl.2015.09.038>

496 Jaccard, S.L., Galbraith, E.D., 2012. Large climate-driven changes of oceanic oxygen
497 concentrations during the last deglaciation. *Nat. Geosci.* 5, 151–156.
498 <https://doi.org/10.1038/ngeo1352>

499 Jaccard, S.L., Galbraith, E.D., Martinez-García, A., Anderson, R.F., 2016. Covariation of
500 deep Southern Ocean oxygenation and atmospheric CO₂ through the last ice age. *Nature*
501 530, 207–10. <https://doi.org/10.1038/nature16514>

502 Kaufman, A., Broecker, W., 1965. Comparison of ²³⁰Th and ¹⁴C ages for carbonate materials
503 from lakes Lahontan and Bonneville. *J. Geophys. Res.* 70, 4039–4054.

504 Keller, N.B., 1976. The deep-sea madreporarian corals of the genus *Fungiacyathus* from the
505 Kurile-Kamchatka, Aleutian Trenches and other regions of the world oceans. *Tr. Inst.*
506 *Okeanol.* 99, 31–44.

507 Kitahara, M. V., Cairns, S.D., Miller, D.J., 2010. Monophyletic origin of Caryophyllia
508 (Scleractinia, Caryophylliidae), with descriptions of six new species. *Syst. Biodivers.* 8,
509 91–118. <https://doi.org/10.1080/14772000903571088>

510 Kohfeld, K.E., Chase, Z., 2017. Temporal evolution of mechanisms controlling ocean carbon
511 uptake during the last glacial cycle. *Earth Planet. Sci. Lett.* 472, 206–215.
512 <https://doi.org/10.1016/j.epsl.2017.05.015>

513 Kohfeld, K.E., Harrison, S.P., Que, C. Le, Anderson, R.F., 2005. Role of marine biology in
514 glacial-interglacial CO₂ cycles. *Science* 308, 74–78.
515 <https://doi.org/10.1126/science.1105375>

516 Labracherie, M., Labeyrie, L.D., Duprat, J., Bard, E., Arnold, M., Pichon, J.-J., Duplessy,
517 J.C., 1989. The last deglaciation in the Southern Ocean. *Paleoceanography* 4, 629–638.
518 <https://doi.org/10.1029/PA004i006p00629>

519 Linnaeus, C., 1758. *Systema naturæ per regna tria naturæ, secundum classes, ordines, genera,*
520 *species, cum characteribus, differentiis, synonymis, locis. Tomus I. Laurentii Salvii,*
521 *Holmiæ.*

522 Lomitschka, M., Mangini, A., 1999. Precise Th/U-dating of small and heavily coated samples
523 of deep sea corals. *Earth Planet. Sci. Lett.* 170, 391–401. <https://doi.org/10.1016/S0012->
524 821X(99)00117-X

525 Lunden, J.J., McNicholl, C.G., Sears, C.R., Morrison, C.L., Cordes, E.E., 2014. Acute
526 survivorship of the deep-sea coral *Lophelia pertusa* from the Gulf of Mexico under
527 acidification, warming, and deoxygenation. *Front. Mar. Sci.* 1, 1–12.
528 <https://doi.org/10.3389/fmars.2014.00078>

529 Lutjeharms, J.R.E., Van Ballegooyen, R.C., 1988. The retroflection of the Aghulas Current. *J.*
530 *Phys. Oceanogr.* 18, 1570–1583.

531 Mangini, A., Godoy, J.M., Godoy, M.L., Kowsmann, R., Santos, G.M., Ruckelshausen, M.,
532 Schroeder-Ritzrau, A., Wacker, L., 2010. Deep sea corals off Brazil verify a poorly
533 ventilated Southern Pacific Ocean during H2, H1 and the Younger Dryas. *Earth Planet.*
534 *Sci. Lett.* 293, 269–276. <https://doi.org/10.1016/j.epsl.2010.02.041>

535 Marcott, S.A., Bauska, T.K., Buizert, C., Steig, E.J., Rosen, J.L., Cuffey, K.M., Fudge, T.J.,
536 Severinghaus, J.P., Ahn, J., Kalk, M.L., McConnell, J.R., Sowers, T., Taylor, K.C.,
537 White, J.W.C., Brook, E.J., 2014. Centennial-scale changes in the global carbon cycle
538 during the last deglaciation. *Nature* 514, 616–9. <https://doi.org/10.1038/nature13799>

539 Marenzeller, E.V., 1904. Reports on dredging operations of the west coast of central America
540 and Galapagos by the U.S. Fish Commission Steamer ‘Albatross’ during 1891:
541 Steinkorallen und Hydro-Korallen. *Bull. Museum Comp. Zool.* 43, 75–87.

542 Margolin, A.R., Robinson, L.F., Burke, A., Waller, R.G., Scanlon, K.M., Roberts, M.L.,
543 Auro, M.E., van de Flierdt, T., 2014. Temporal and spatial distributions of cold-water
544 corals in the Drake Passage: Insights from the last 35,000 years. *Deep. Res. Part II Top.*
545 *Stud. Oceanogr.* 99, 237–248. <https://doi.org/10.1016/j.dsr2.2013.06.008>

- 546 Marshall, J., Speer, K., 2012. Closure of the meridional overturning circulation through
547 Southern Ocean upwelling. *Nat. Geosci.* 5, 171–180. <https://doi.org/10.1038/ngeo1391>
- 548 Martínez-Botí, M.A., Marino, G., Foster, G.L., Ziveri, P., Henehan, M.J., Rae, J.W.B.,
549 Mortyn, P.G., Vance, D., Marino, G., Ziveri, P., Henehan, M.J., Foster, G.L., Vance, D.,
550 Martínez-Botí, M.A., Rae, J.W.B., 2015. Boron isotope evidence for oceanic carbon
551 dioxide leakage during the last deglaciation. *Nature* 518, 219–222.
552 <https://doi.org/10.1038/nature14155>
- 553 Martínez-García, A., Sigman, D.M., Ren, H., Anderson, R.F., Straub, M., Hodell, D.A.,
554 Jaccard, S.L., Eglinton, T.I., Haug, G.H., 2014. Iron fertilization of the Subantarctic
555 ocean during the last ice age. *Science* 343, 1347–50.
556 <https://doi.org/10.1126/science.1246848>
- 557 Mastumoto, K., Lynch-Stieglitz, J., Anderson, R.F., 2001. Similar glacial and Holocene
558 Southern Ocean hydrography. *Paleoceanography* 16, 445–454.
- 559 McCave, I.N., Crowhurst, S.J., Kuhn, G., Hillenbrand, C.D., Meredith, M.P., 2014. Minimal
560 change in Antarctic Circumpolar Current flow speed between the last glacial and
561 Holocene. *Nat. Geosci.* 7, 113–116. <https://doi.org/10.1038/ngeo2037>
- 562 Mccave, I.N., Kiefer, T., Thornalley, D.J.R., Elderfield, H., 2005. Deep flow in the
563 Madagascar-Mascarene Basin over the last 150 000 years. *Philos. Trans. R. Soc. A*
564 *Math. Phys. Eng. Sci.* 363, 81–99. <https://doi.org/10.1098/rsta.2004.1480>
- 565 Miller, K.J., Rowden, A.A., Williams, A., Haussermann, V., 2011. Out of their depth?
566 isolated deep populations of the cosmopolitan coral *Desmophyllum dianthus* may be
567 highly vulnerable to environmental change. *PLoS One* 6.
568 <https://doi.org/10.1371/journal.pone.0019004>
- 569 Milne Edwards, H., Haime, J., 1848. *Recherches sur les polypiers. Deuxième mémoire.*

- 571 Monnin, E., Indermühle, A., Dällenbach, A., Flückiger, J., Stauffer, B., Stocker, T.F.,
572 Raynaud, D., Barnola, J.-M., 2001. Atmospheric CO₂ concentrations over the Last
573 Glacial Termination. *Science* 291, 112–114.
574 <https://doi.org/10.1126/science.291.5501.112>
- 575 Montero-Serrano, J.-C., Frank, N., Tisnérat-Laborde, N., Colin, C., Wu, C.-C., Lin, K., Shen,
576 C.-C., Copard, K., Orejas, C., Gori, A., De Mol, L., Van Rooij, D., Reverdin, G.,
577 Douville, E., 2013. Decadal changes in the mid-depth water mass dynamic of the
578 Northeastern Atlantic margin (Bay of Biscay). *Earth Planet. Sci. Lett.* 364, 134–144.
579 <https://doi.org/10.1016/j.epsl.2013.01.012>
- 580 Moseley, H.N., 1881. Report on Certain Hydroid, Alcyonarian, and Madreporarian Corals
581 Procured during the Voyage of H. M. S. Challenger, in the Years 1873-1876. *Zoology* 2,
582 1–248.
- 583 Naumann, M.S., Orejas, C., Wild, C., Ferrier-Pages, C., 2011. First evidence for zooplankton
584 feeding sustaining key physiological processes in a scleractinian cold-water coral. *J.*
585 *Exp. Biol.* 214, 3570–3576. <https://doi.org/10.1242/jeb.061390>
- 586 Ninnemann, U.S., Charles, C.D., 2002. Changes in the mode of Southern Ocean circulation
587 over the last glacial cycle revealed by foraminiferal stable isotopic variability. *Earth*
588 *Planet. Sci. Lett.* 201, 383–396. [https://doi.org/10.1016/S0012-821X\(02\)00708-2](https://doi.org/10.1016/S0012-821X(02)00708-2)
- 589 Parrenin, F., Masson-Delmotte, V., Köhler, P., Raynaud, D., Paillard, D., Schwander, J.,
590 Barbante, C., Landais, A., Wegner, A., Jouzel, J., Kohler, P., Raynaud, D., Paillard, D.,
591 Schwander, J., Barbante, C., Landais, A., Wegner, A., Jouzel, J., 2013. Synchronous
592 change of atmospheric CO₂ and Antarctic temperature during the last deglacial warming.
593 *Science* 339, 1060–1063. <https://doi.org/10.1126/science.1226368>

594 Plancherel, Y., 2012. A study of the ocean's water masses using data and models. Princeton
595 University.

596 Pollard, R.T., Venables, H.J., Read, J.F., Allen, J.T., 2007. Large-scale circulation around the
597 Crozet Plateau controls an annual phytoplankton bloom in the Crozet Basin. *Deep. Res.*
598 *Part II Top. Stud. Oceanogr.* 54, 1915–1929. <https://doi.org/10.1016/j.dsr2.2007.06.012>

599 Rae, J.W., Burke, A., Robinson, L.F., Adkins, J.F., Chen, T., Cole, C., Greenop, R., Li, T.,
600 Littley, E., Nita, D.C., Stewart, J.A., Taylor, B., 2018. CO₂ storage and release in the
601 deep Southern Ocean on millennial to centennial timescales. *Nature* 562, 569–573.
602 <https://doi.org/10.1038/s41586-018-0614-0>

603 Read, J.F., Lucas, M.I., Holley, S.E., Pollard, R.T., 2000. Phytoplankton, nutrients and
604 hydrography in the frontal zone between the Southwest Indian Subtropical gyre and the
605 Southern Ocean. *Deep. Res. Part I Oceanogr. Res. Pap.* 47, 2341–2368.
606 [https://doi.org/10.1016/S0967-0637\(00\)00021-2](https://doi.org/10.1016/S0967-0637(00)00021-2)

607 Read, J.F., Pollard, R., 2017. An introduction to the physical oceanography of six seamounts
608 in the southwest Indian Ocean. *Deep. Res. Part II Top. Stud. Oceanogr.* 136, 44–58.
609 <https://doi.org/10.1016/j.dsr2.2015.06.022>

610 Reimer, P.J., Baille, M.G.L., Bard, E., Bayliss, A., Beck, J.W., Blackwell, P.G., Bronk
611 Ramsey, C., Buck, C.E., Burr, G.S., 2009. INTCAL09 and MARINE09 radiocarbon age
612 calibration curves, 0-50,000 years cal BP. *Radiocarbon* 51, 1111–1150.

613 Roberts, J., Gottschalk, J., Skinner, L.C., Peck, V.L., Kender, S., Elderfield, H., Waelbroeck,
614 C., Vázquez Riveiros, N., Hodell, D.A., Gottschalk, J., Elderfield, H., Peck, V.L.,
615 Skinner, L.C., Kender, S., Hodell, D.A., Roberts, J., Vázquez Riveiros, N., 2016.
616 Evolution of South Atlantic density and chemical stratification across the last
617 deglaciation. *Proc. Natl. Acad. Sci.* 113, 514–519.

- 619 Roberts, J., McCave, I.N., McClymont, E.L., Kender, S., Hillenbrand, C.D., Matano, R.,
620 Hodell, D.A., Peck, V.L., 2017. Deglacial changes in flow and frontal structure through
621 the Drake Passage. *Earth Planet. Sci. Lett.* 474, 397–408.
622 <https://doi.org/10.1016/j.epsl.2017.07.004>
- 623 Roberts, J.M., Wheeler, A.J., Friewald, A., 2006. Reefs of the deep: the biology and geology
624 of cold-water coral ecosystems. *Science* 312, 543–7. <https://doi.org/DOI>
625 10.1126/science.1119861
- 626 Roberts, J.M., Wheeler, A.J., Friewald, A., Cairns, S.D., 2009. *Cold-Water Corals: The*
627 *Biology and Geology of Deep-Sea Coral Habitats*. Cambridge University Press,
628 Cambridge.
- 629 Robinson, L.F., Adkins, J.F., Frank, N., Gagnon, A.C., Prouty, N.G., Brendan Roark, E., van
630 de Flierdt, T., 2014. The geochemistry of deep-sea coral skeletons: A review of vital
631 effects and applications for palaeoceanography. *Deep. Res. Part II Top. Stud. Oceanogr.*
632 99, 184–198. <https://doi.org/10.1016/j.dsr2.2013.06.005>
- 633 Rogers, A.D., Taylor, M.L., 2011. Benthic biodiversity of seamounts in the southwest Indian
634 Ocean: Cruise Report – R/V James Cook 066 Southwest Indian Ocean Seamounts
635 expedition.
- 636 Romahn, S., MacKensen, A., Groeneveld, J., Pätzold, J., 2014. Deglacial intermediate water
637 reorganization: New evidence from the Indian Ocean. *Clim. Past* 10, 293–303.
638 <https://doi.org/10.5194/cp-10-293-2014>
- 639 Sabine, C.L., Key, R.M., Feely, R.A., Greeley, D., 2002. Inorganic carbon in the Indian
640 Ocean: Distribution and dissolution processes. *Global Biogeochem. Cycles* 16, 15-1-15–
641 18. <https://doi.org/10.1029/2002GB001869>

- 643 Shen, C.-C., Li, K.-S., Sieh, K., Natawidjaja, D., Cheng, H., Wang, X., Edwards, R.L., Lam,
644 D.D., Hsieh, Y.-T., Fan, T.-Y., Meltzner, A.J., Taylor, F.W., Quinn, T.M., Chiang, H.-
645 W., Kilbourne, K.H., 2008. Variation of initial $^{230}\text{Th}/^{232}\text{Th}$ and limits of high precision
646 U–Th dating of shallow-water corals. *Geochim. Cosmochim. Acta* 72, 4201–4223.
647 <https://doi.org/10.1016/j.gca.2008.06.011>
- 648 Shen, C.-C., Wu, C.-C., Cheng, H., Lawrence Edwards, R., Hsieh, Y.-T., Gallet, S., Chang,
649 C.-C., Li, T.-Y., Lam, D.D., Kano, A., Hori, M., Spötl, C., 2012. High-precision and
650 high-resolution carbonate ^{230}Th dating by MC-ICP-MS with SEM protocols. *Geochim.*
651 *Cosmochim. Acta* 99, 71–86. <https://doi.org/10.1016/j.gca.2012.09.018>
- 652 Shen, G.T., Boyle, E.A., 1988. Determination of lead, cadmium and other trace metals in
653 annually-banded corals. *Chem. Geol.* 67, 47–62. [https://doi.org/10.1016/0009-](https://doi.org/10.1016/0009-2541(88)90005-8)
654 [2541\(88\)90005-8](https://doi.org/10.1016/0009-2541(88)90005-8)
- 655 Siani, G., Michel, E., De Pol-Holz, R., DeVries, T., Lamy, F., Carel, M., Isguder, G.,
656 Dewilde, F., Laurantou, A., 2013. Carbon isotope records reveal precise timing of
657 enhanced Southern Ocean upwelling during the last deglaciation. *Nat. Commun.* 4, 1–9.
658 <https://doi.org/10.1038/ncomms3758>
- 659 Sigman, D.M., Hain, M.P., Haug, G.H., 2010. The polar ocean and glacial cycles in
660 atmospheric CO_2 concentration. *Nature* 466, 47–55. <https://doi.org/10.1038/nature09149>
- 661 Sikes, E.L., Howard, W.R., Samson, C.R., Mahan, T.S., Robertson, L.G., Volkman, J.K.,
662 2009. Southern Ocean seasonal temperature and Subtropical Front movement on the
663 South Tasman Rise in the late Quaternary. *Paleoceanography* 24, 1–13.
664 <https://doi.org/10.1029/2008PA001659>
- 665 Skinner, L.C., Fallon, S., Waelbroeck, C., Michel, E., Barker, S., 2010. Ventilation of the

666 deep Southern Ocean and deglacial CO₂ rise. *Science* 328, 1147–1151.
667 <https://doi.org/10.1126/science.1183627>

668 Sokolov, S., Rintoul, S.R., 2009. Circumpolar structure and distribution of the antarctic
669 circumpolar current fronts: 1. Mean circumpolar paths. *J. Geophys. Res. Ocean.* 114, 1–
670 19. <https://doi.org/10.1029/2008JC005108>

671 Spooner, P.T., Chen, T., Robinson, L.F., Coath, C.D., 2016. Rapid uranium-series age
672 screening of carbonates by laser ablation mass spectrometry. *Quat. Geochronol.* 31, 28–
673 39. <https://doi.org/10.1016/j.quageo.2015.10.004>

674 Squires, D.F., 1961. Deep Sea Corals Collected by the Lamont Geological Observatory:
675 Scotia Sea Corals. American Museum of Natural History.

676 Stanley, G.D., Cairns, S.D., 1988. Constructional azooxanthellate coral communities: An
677 overview with implications for the fossil record. *Palaios* 3, 233.
678 <https://doi.org/10.2307/3514534>

679 Stenni, B., Buiron, D., Frezzotti, M., Albani, S., Barbante, C., Bard, E., Barnola, J.M.M.,
680 Baroni, M., Baumgartner, M., Bonazza, M., Capron, E., Castellano, E., Chappellaz, J.,
681 Delmonte, B., Falourd, S., Genoni, L., Iacumin, P., Jouzel, J., Kipfstuhl, S., Landais, A.,
682 Lemieux-Dudon, B., Maggi, V., Masson-Delmotte, V., Mazzola, C., Minster, B.,
683 Montagnat, M., Mulvaney, R., Narcisi, B., Oerter, H., Parrenin, F., Petit, J.R.R., Ritz, C.,
684 Sarchilli, C., Schilt, A., Schüpbach, S., Schwander, J., Selmo, E., Severi, M., Stocker,
685 T.F.F., Udisti, R., 2011. Expression of the bipolar see-saw in Antarctic climate records
686 during the last deglaciation. *Nat. Geosci.* 4, 46–49. <https://doi.org/10.1038/ngeo1026>

687 Stenni, B., Masson-Delmotte, V., Johnsen, S., Jouzel, J., Longinelli, A., Monnin, E.,
688 Röthlisberger, R., Selmo, E., 2001. An oceanic cold reversal during the last deglaciation.
689 *Science* 293, 2074–2077. <https://doi.org/10.1126/science.1059702>

690 Stephens, B.B., Keeling, R.F., 2000. The influence of Antarctic sea ice on glacial-interglacial
691 CO₂ variations. *Nature* 404, 171–174. <https://doi.org/10.1038/35004556>

692 Thiagarajan, N., Gerlach, D., Roberts, M.L., Burke, A., McNichol, A., Jenkins, W.J., Subhas,
693 A. V., Thresher, R.E., Adkins, J.F., 2013. Movement of deep-sea coral populations on
694 climatic timescales. *Paleoceanography* 28, 227–236. <https://doi.org/10.1002/palo.20023>

695 Thresher, R.E., Tilbrook, B., Fallon, S., Wilson, N.C., Adkins, J., 2011. Effects of chronic
696 low carbonate saturation levels on the distribution, growth and skeletal chemistry of
697 deep-sea corals and other seamount megabenthos. *Mar. Ecol. Prog. Ser.* 442, 87–96.
698 <https://doi.org/10.3354/meps09400>

699 van Aken, H.M., Ridderinkhof, H., de Ruijter, W.P.M., 2004. North Atlantic deep water in
700 the south-western Indian Ocean. *Deep Sea Res. Part I Oceanogr. Res. Pap.* 51, 755–776.
701 <https://doi.org/10.1016/j.dsr.2004.01.008>

702 van de Flierdt, T., Robinson, L.F., Adkins, J.F., 2010. Deep-sea coral aragonite as a recorder
703 for the neodymium isotopic composition of seawater. *Geochim. Cosmochim. Acta* 74,
704 6014–6032. <https://doi.org/10.1016/j.gca.2010.08.001>

705 WAIS Divide Project Members, 2015. Precise inter-polar phasing of abrupt climate change
706 during the last ice age. *Nature* 520, 661–665. <https://doi.org/10.1038/nature14401>

707 Wang, X.T., Sigman, D.M., Prokopenko, M.G., Adkins, J.F., Robinson, L.F., Hines, S.K.,
708 Chai, J., Studer, A.S., Martínez-García, A., Chen, T., Haug, G.H., 2017. Deep-sea coral
709 evidence for lower Southern Ocean surface nitrate concentrations during the last ice age.
710 *Proc. Natl. Acad. Sci.* 114, 3352–3357. <https://doi.org/10.1073/pnas.1615718114>

711 Watling, L., Guinotte, J., Clark, M.R., Smith, C.R., 2013. A proposed biogeography of the
712 deep ocean floor. *Prog. Oceanogr.* 111, 91–112.
713 <https://doi.org/10.1016/j.pocean.2012.11.003>

714 Yu, J., Broecker, W.S., Elderfield, H., Jin, Z., McManus, J.F., Zhang, F., 2010. Loss of
715 carbon from the deep sea since the Last Glacial Maximum. *Science* 330, 1084–1087.

716 Zibrowius, H., 1980. Les scléactiniaires de la Méditerranée et de l'Atlantique nord-oriental.
717 Mémoires de l'Institut Océanographique, Monaco 11, 1–284.

718

719 **Contributions**

720 All authors have contributed to this work. Their individual roles are detailed as follows: NP
721 carried out sample identifications, prepared samples for dating, interpreted the data, and
722 wrote the manuscript with input from all authors; ADR and MLT carried out sample
723 collection on the JC066 cruise, following the request of TvdF, and assisted with video
724 analysis of sample locations; TC led the laser ablation and isotope dilution U-series dating
725 and data processing, and Tao Li carried out part of the isotope dilution U-series analyses,
726 under the supervision of LFR at the University of Bristol; NS provided training and guidance
727 on taxonomic analysis of the specimens at the Natural History Museum and edits on the
728 manuscript; LFR, TvdF, DJW and SHL aided discussions on data interpretation. All authors
729 edited and have approved the final manuscript.

730 **Conflicts of interest**

731 Declarations of interest: none.

732 **Notes for editor**

733 Please use colour for all figures in print.

Manuscript entitled ‘Temporal distribution and diversity of cold-water corals in the southwest Indian Ocean over the past 25,000 years’.

Highlights

- First described southern Indian Ocean subfossil cold-water coral collection
- Eight new species to the region identified
- Dated using rapid laser ablation and isotope dilution uranium series techniques
- Abundance peak during late deglacial a possible response to optimal ocean chemistry
- Striking similarities in temporal distribution to other Southern Ocean collections